A PC-Based System for the Determination of Harmonics and Intermodulation Products in Nonlinear Circuits

by

Rizwan Ali Tiwana

A Thesis Presented to the

FACULTY OF THE COLLEGE OF GRADUATE STUDIES

KING FAHD UNIVERSITY OF PETROLEUM & MINERALS

DHAHRAN, SAUDI ARABIA

In Partial Fulfillment of the
Requirements for the Degree of

MASTER OF SCIENCE

In

ELECTRICAL ENGINEERING

December, 1994

A PC-Based System for the Determination of Harmonics and Intermodulation Products in Nonlinear Circuits

BY

Rizwan Ali Tiwana

A Thesis Presented to the

FACULTY OF THE COLLEGE OF GRADUATE STUDIES

KING FAHD UNIVERSITY OF PETROLEUM & MINERALS

DHAHRAN, SAUDI ARABIA

In Partial Fulfillment of the
Requirements for the Degree of

MASTER OF SCIENCE
In
Electrical Engineering

December 1994

KING FAHD UNIVERSITY OF PETROLEUM AND MINERALS
DHAHRAN, SAUDI ARABIA

This thesis, written by

Rizwan Ali Tiwana

under the direction of his Thesis Advisor, and approved by his Thesis committee, has been presented to and accepted by the Dean, College of Graduate Studies, in partial fulfillment of the requirements for the degree of

MASTER OF SCIENCE IN ELECTRICAL ENGINEERING

Thesis Committee:

Dr. M. T. Abuelma'atti (Chairman)

Dr. A. R. K. Al-Ali (Co-Chairman)

Dr. I. M. Naqvi (Member)

Dr. Z. J. Saati (Member)

Dr. J. Zrida (Member)

Dr. A. M. Al-Shehri
Chairman
Electrical Engineering Department

Dr. Ala H. Rabeh
Dean, College of Graduate Studies

Date: 31.1.95

Dedicated to

My Parents & Masuma

Acknowledgment

Acknowledgement is due to King Fahd University of Petroleum and Minerals for providing support to this work. My deep appreciation goes to my major thesis advisor Dr. M. T. Abuelma'atti for his constant help and guidance he provided throughout the course of this work.

Thanks are due to my thesis co-advisor Dr. Al-Ali and committee members Dr. Naqvi, Dr. Saati and Dr. Zrida for their interest and co-operation. In particular, I owe a considerable debt to Dr. Al-Ali for his invalulable support, help and encouragement.

I am also grateful to the department chairman, Dr. Abdallah Al-Shehri and other faculty members for their support

I would also like to acknowledge the support that I received from Fahim Shafi during the thesis and its compilation. Another word of thanks must go to all my friends on the campus especially (in alphabatical order), Adnan, Asif, Atif, Azher, Firoz, Haroun, Irfan, and Imtiaz who made my stay at KFUPM a pleasant experience.

I also remain grateful to Lab-Technicians Mr. Farazi and Mr. Shams for their support and cooperation.

Contents

List of Tables

List of Figures

Abstract

Name: Rizwan Ali Tiwana

Title: A PC-Based System for the Determination of Harmonics & Intermodulation Products in Nonlinear Circuits

Major Field: Electrical Engineering

Date of Degree: December, 1994

In this thesis, a PC based integrated system has been designed and implemented. The system has been used to predict the amplitudes of intermodulation products (IMP) at the output of nonlinear circuits exhibiting amplitude nonlinearity. The input-output characteristics are measured and stored automatically. These characteristics are then used to simulate the device behavior. A frequency dependent model has been implemented for computation of intermodulation products. Fourier series approximation routines are used for characteristic approximation and generation of frequency dependent parameters. The model determines amplitudes of intermodulation products in terms of Bessel functions

Master of Science Degree
King Fahd University of Petroleum and Minerals
Dhahran, Saudi Arabia
December 1994

خلاصة الرسالة

الاسم : رضوان على تيوانا

عنوان الرسالة : حساب التوافقيات و التضمين التبادلى فى الدوائر غير الخطية باستخدام الحاسب الشخصى

التخصص : الهندسة الكهربائية

تاريخ الشهادة : ديسمبر ١٩٩٤م

فى هذه الاطروحه تم تصميم و تنفيذ نظام لحساب سعه التوافقيات و التضمين التبادلى الناتجه من الدوائر غير الخطية باستخدام الحاسب الشخصى. ويعتمد النظام المقترح على قياس العلاقه بين الداخل و الخارج من الدائره و من ثم تخزين المعلومات آليا واستخدامها لحساب نموذج رياضى للدائره غير الخطية. وهذا النموذج يأخذ فى الحسبان اعتماد العلاقه بين الداخل والخارج على الذبذبه. وقد استخدمت داله "فورير" لتمثيل العلاقه بين الداخل و الخارج و من ثم حساب معاملاتها المعتمده على الذبذبه. وباستخدام هذا النموذج يمكن حساب سعه التوافقيات و التضمين التبادلى بدلاله دوال "بسل".

درجة الماجستير فى العلوم

جامعة الملك فهد للبترول و المعادن

الظهران – المملكة العربية السعودية

ديسمبر ١٩٩٤م

Chapter 1

Introduction

1.1 Overview

The input-output characteristics (transfer charactersitics) of most of the electronic circuits are nonlinear. For a device (e.g, amplifier) operated by two power supplies the output voltage cannot exceed a positive limit and cannot decrease below a specified negative limit. Each of the two saturation levels are usually within a few volts of the corresponding power supplies. The circuit behaviour is not only dependent on the amplitude of the input applied but also on the frequency of the input signal. The circuit can exhibit nonlinear behavior when :

- Magnitude of the input signal exceeds a certain limit.
- Frequency of the input signal is sufficiently high or low (depending on the configuration of the device).

A linear system characteristics can be represented by an equation of the form

$$y = ax$$

where y is the output, a the scaling factor and x is the input to the device, the scaling factor can be frequency dependent. A device whose characteristics are approximated by a polynomial of degree higher than one is nonlinear (e.g, $y = ax + bx^2$).

Harmonics are generated when single tone signals are applied to nonlinear devices. If the characteristics are approximated by the equation :

$$y = ax + bx^2$$

and the input to the device is

$$x = A\sin(2\pi f_o t)$$

then the output is given by the following equation

$$y = aA\sin(2\pi f_o t) + bA^2\sin^2(2\pi f_o t)$$

The output will contain a DC component as well as carrier f_o and harmonic $2f_o$.

Intermodulation products (IMPs) are frequencies other than carriers generated at the output when two or more frequencies are applied simultaneously to a device having nonlinear characteristics. For example, the application of three frequencies, f_1, f_2, f_3, simulatneously to a device whose characteristics are given by the third order polynomial:

$$y = ax + bx^2 + cx^3 \tag{1.1}$$

gives rise to a spectrum consisting of up to 32 frequencies between DC and sum of the input frequencies. When an IMP is generated, at a frequency that is within or near the band of operation, the performance of the device is degraded. Hence it is frequently valuable in design of communication systems and equipment to have a real time prediction of the likely spectrum of the output signals including the IMPs.

Computer simulation is often used to determine the likely output spectrum and device behavior. In order to simulate, it is necessary to have models characterizing the nonlinear device. It is essential that models for these nonlinearities be as accurate as possible so that meaningful results are obtained. The simulation results can help

the designer take preventive measures ensuring proper operation of the device. A simulation process involves following steps:

- Measuring device characteristics.
- Approximating the characteristics.
- Modelling the device behavior.
- Calculating IMP frequencies.
- Predicting output amplitudes at IMPs.
- Validating the results.

1.2 Literature Review

Electronic device manufacturers have developed detailed *low level* models (especially for amplifiers) that typically involve solving a set of simultaneous, possibly nonlinear, equations by numerical methods for the required device output [1]. Such detailed models are far too time consuming to be useful in a system simulation where the amplifier is just one of the many devices. Hence a higher level model, that converts an input waveform to the correct output waveform without unnecessarily resorting to the fundamental physics of the device is needed. For linear systems, transfer function is such a model. General input-output type models for nonlinear systems with memory (frequency dependent systems) have been proposed, such as Volterra series, describing functions and rational polynomials. But none as of yet have seemed to provide an efficient enough implementation with easily measured parameters, so that they could be used and accepted as readily as the transfer function is for linear systems.

1.2.1 Memoryless Nonlinear Amplifiers

For nonlinear amplifiers which do not exhibit any significant frequency selective effects, the theory is well developed. These types of amplifiers can be sufficiently described by an instantaneous memory-less model [2]. The nonlinearities exhibited by these amplifiers can be categorized into output amplitude versus input amplitude nonlinearity (AM/AM) and output phase versus input amplitude nonlinearity (AM/PM effect). The model is characterised by a complex functional relationship between the input and output envelope. Blachman and Benedetto [3, 4] have shown that the functions describing AM/AM and AM/PM nonlinearities depend only on the modulus of the input envelope. This model can be implemented in either the serial envelope phase version, Fig. 1.1, or the parallel inphase-quadrature format, Fig. 1.2.

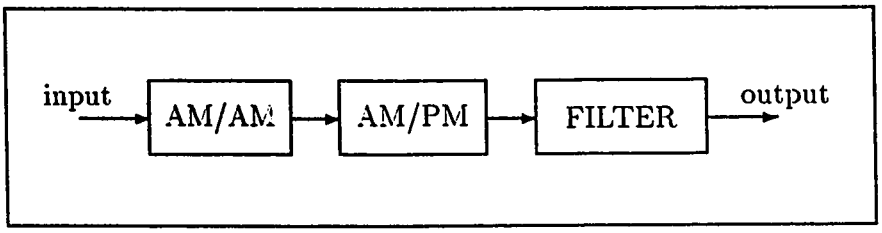

Figure 1.1: Envelope and Phase Model Format of a Memoryless System

In Fig. 1.2, S_I represents the inphase amplitude nonlinearity (having the same phase as that of the input signal) and S_Q is the quadrature nonlinearity (90° out of phase with the input signal). The AM/AM and AM/PM functions can be measured easily through single sine-wave, swept tone measurements which, along with the model's inherent simplicity, make this model quite attractive.

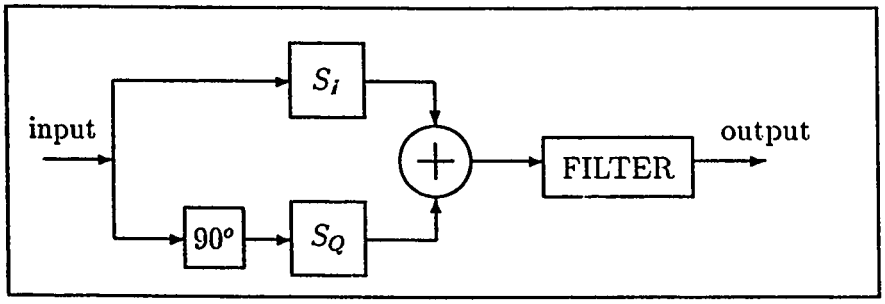

Figure 1.2: Inphase and Quadrature Memoryless System

1.2.2 Nonlinear Amplifier with Memory

The Volterra series [5] approach to modelling amplifiers with frequency selectivity is appealing due to its clear relationship to a linear system's impulse response. A Volterra series is a Taylor series with memory described by

$$Y(t) = \sum_{n=1}^{\infty} Y_n(t) \tag{1.2}$$

Here the system is assumed to have no constant (dc) response. Each term of order 'n' is described by an n-fold convolution as

$$Y_n(t) = \int_{-\infty}^{\infty} \dots \int_{-\infty}^{\infty} h(T_1, T_2, ..., T_n)\, x(t - T_1) \dots x(t - T_n)\, dT_1 \dots dT_n \tag{1.3}$$

In equation (1.3) Y is the system output, h is the system's impulse response and x is the input to the systen.. The first order term is the usual linear system response. An immediate problem with the Volterra series is the justification of truncating the series at some order.

Boyd [6] has demostrated the validity of a truncation procedure for a large class of systems that he calls *fading memory systems*. The other major problem with Volterra series is the complexity of the measurements needed to identify the kernels (Volterra series coefficients). The truncation procedure along with the complexity of

the actual model make a Volterra series impractical for all but very few applications in which the complexity and cost can be justified [6]. Chang [7] has suggested a simplification to the Volterra series approach which assumes that the kernels are single-frequency dependent.

Hu et al. [8] have proposed a third order Volterra series model for microwave FET amplifiers. They have made the assumption that a frequency independent relationship exists between the drain current and gate voltage, as well as between the drain current and the drain to source voltage. While this model is useful for FETs in specific configurations it is difficult to generalize the model to any technology or configuration, for Travelling Wave Tubes (TWT) such current voltage relationships do not exist hence the model is inapplicable.

1.2.3 Heiter's Power Series Model

Heiter [9] has introduced a power series model in which each term of the power series is delayed by a different amount. Heiter presents data to show that the model is useful for intermodulation prediction. However, the performance for general modulated inputs is not discussed. This model can be viewed as a simplification of the general Volterra series although the simplification is difficult to justify [10].

1.2.4 Hetrakul's Quadrature Model

Nonlinearities exhibited by a band-pass amplifier (specifically Travelling Wave Tube (TWT)) were modelled by Eric [11] using the power series method. The same model was extended by Hetrakul and Taylor [12] in the form of a quadrature model. The model since then has formed the basis for many proposed modifications. The TWT amplifier generally introduces two kinds of nonlinearities: first there is a nonlinear amplitude (AM/AM) relationship and secondly, there is a non-linear phase relationship (AM/PM), shown in Fig. 1.3.

This was the first time that nonlinear phase effects were incorporated in the amplifier's model. The model consisted of two envelope nonlinearities, one in the inphase and other in the quadrature path. Modified Bessel functions of the first kind and second order were used to approximate these nonlinearities. Unlike the power series method of Eric [11] this Bessel function approximation needs only a few coefficients to give a good fit to the TWT nonlinearities, and, further it circumvents the anamalous behaviour observed at large input voltages, when power-series approximations were used. The model implies that the TWT amplifier characteristics are independent of frequency over the frequency band of interest. However when broadband signals are involved, or in systems incorporating a wide-band TWT amplifier and relatively narrow-band components the model fails to justify the results because here a frequency dependent model is needed.

1.2.5 Poza Et Al. Model

This model appears to be the first attempt to extend the frequency independent (memory less) model which is specifically useful for computer simulation. The model is based on the observation that the curves for amplitude (AM/AM) nonlinearity measured at different test frequencies maintain nearly the same shape when plotted on a dB to dB scale. Thus the AM/AM curves for various frequencies were obtained from a single curve with appropriate horizontal and vertical shifts applied. The shifts on dB scale are equivalent to multiplication by scaling factors on real scales and thus they correspond to frequency dependent scaling on both scales (abscissa and ordinate). This scaling was implemented by amplitude only filters preceeding and following the AM/AM nonlinearity. The idea is illustrated in Fig. 1.4. $H_{a1}(f)$ and $H_{a2}(f)$ are pure amplitude filters. $H_{a1}(f)$ implements the Horizontal shift (shift on $x-axis$) and $H_{a2}(f)$ implements the vertical shift (shift on $y-axis$) of input power vs output power graph. The AM/PM curves for different frequencies were also

observed to maintain shapes for different frequencies. This time the shifts are visible on phase vs dB scale and thus the vertical shifts are implemented with a pure phase filter, Fig. 1.5. $H_p(f)$ is a pure amplitude filter and $\Phi_p(f)$ is a pure phase filter. $H_p(f)$ implements the Horizontal shift (shift on $x-axis$) and $\Phi_p(f)$ implements the vertical shift (shift on $y-axis$) of input power vs output phase graph. A block diagram of the complete implementation as reported by [10] is shown in Fig. 1.6.

The actual AM/AM and AM/PM curves do not exactly maintain their shapes [10]. The attempt by Poza [13] was to compensate for this through elaborate fitting procedure that found a curve which best fits all the measured versions. The procedure also determined the best shift values for each frequency. The fitting procedure seems to be quite complicated and it may be adequate to just use a curve measured at a nominal frequency and determine the best shifts based on a minimum mean square fit to measured data [10]. The model should give good results for single tone unmodulated inputs by virtue of its construction, and its accuracy, for such unmodulated tones, relies only on the validity of the constant shape AM/AM and AM/PM curve assumption. The behavior of the model for multi tone signal is unclear [10].

1.2.6 Saleh's Model

Saleh [14] proposed a simple frequency independent model in the inphase and quadrature format as depicted in Fig. 1.2. He picked two parameter, rational functions of the form

$$P(r) = \frac{\alpha_p r}{1 + \beta_p r^2} \;\&\; Q(r) = \frac{\alpha_q r^3}{(1 + \beta_q r^2)^2} \tag{1.4}$$

Where r is the input envelope magnitude , $P(r)$ and $Q(r)$ are inphase and quadrature nonlinearities which are odd functions of 'r', α, and β are approximation parameters. Saleh also derived equations from a mean square fitting criterion to obtain the model parameters from the measured characteristics. He also proposed an extension of the same model for the frequency dependent case. The extension is based on the

observation that the parameters of above equation can fit AM/AM and AM/PM characteristics measured at any frequency. The coefficients therefore become frequency dependent which is equivalent to adding real filters before and after the inphase and quadrature nonlinearities. The block diagram of implementation is shown in Fig. 1.7.

In Fig. 1.7, $P_o(r)$ and $Q_o(r)$ are frequency independent nonlinearities; the $H's$ and $G's$ are real linear filters, and $\Phi_o(f)$ is a linear all-pass network.

1.2.7 Abuelma'atti's Model

The model proposed by Abuelma'atti [15] is also in the form of the quadrature model. The inphase and quadrature nonlinearities are expanded in terms of first order Bessel functions as :

$$P(r) = \sum_{n=1}^{N} \gamma_{nI} J_1 \left(\frac{n\pi r}{D}\right) \tag{1.5}$$

$$Q(r) = \sum_{n=1}^{N} \gamma_{nQ} J_1 \left(\frac{n\pi r}{D}\right) \tag{1.6}$$

Where 2D is the dynamic range of input, $P(r)$ and $Q(r)$ are the inphase and quadrature nonlinearities, and r is the input envelope amplitude. γ_{nI} and γ_{nQ} provided a minimum mean square fit to the measured nonlinearity curve. These coefficients are made frequency dependent by fitting curves measured at different frequencies via an approximation method. The implementation of frequency dependant coefficients is achieved by cascading nominal coefficients with real filters. A block diagram of implementation is shown in Fig. 1.8. Although the model is more complicated, it has the advantage of not assuming any curve shapes that remain constant from frequency to frequency [10]. For a sufficient number of terms N in the equations (1.5) and (1.6), the summation can represent any measured curve to any desired accuracy. Therefore with different expansion coefficients at different frequencies the

curves can change shape in any arbitrary way. A multitone input signal with arbitrary tone amplitudes will be processed by several parallel connected branches. Each branch consists of a frequency independent amplitude nonlinearity followed by the appropriate filter.

1.3 Problem Definition

The available models that incorporate the frequency selectivity of electronic devices in general and amplifiers in particular are distinguished from one another by the computational complexity and approximation techniques. An integrated system capable of measuring the characteristics, computing and predicting the output amplitudes at IMPs would have to incorporate one of the exsisting models and a facility for determinig the characteristics. Since the whole system will be implemented on a personal computer, attention must be paid to the computational efficiency. The chosen model and the characteristic approximation method must be easily integrable. The system should be able to predict the output amplitudes for any order of nonlinearity desired.

None of the mentioned models have been implemented practically which can be considered as a drawback for all the models. Blum & Jerrichum [10] have done a comparison of available models they, point out that Saleh's model is in some sense the dual to the Poza's model. Where Poza's model is constrained to keep the AM/AM and the AM/PM curves of the constant shape, Saleh's model is constrained to keep the inphase and quadrature curve shapes unaltered as a function of frequency [10]. It is a condition imposed when he (Saleh [14]) requires that both the inphase and quadrature sections of the model factor into frequency independent nonlinearity filter. This implies that as with Poza's model the AM/AM and AM/PM nonlinearities must maintain their shapes on the dB scale. The fact that Saleh has coefficients that are functions of frequency does nothing to alter the situation because he has picked

special forms of functions that allow these coefficients to be factored out into these sandwiching filters, Fig. 1.7. Thus, Saleh's model requires the single tone curves for amplitude nonlinearity and quadrature nonlinearity to maintain their shape for different frequencies. Just as for Poza's model, only horizontal shifts are possible. It can be mathematically shown [10], that constraining the amplitude and phase curves to maintain shape is fundamentally different than requiring the inphase and quadrature nonlinearities to maintain shape. The set of curves generated by one do not completely overlap the curves generated by the other. Therefore even for single tone unmodulated inputs Poza's and Saleh's model will yeild different results. The models will only yield identical results for AM/AM and AM/PM characteristics when abscissae are scaled identically as functions of the frequency.

Accuracy of the two models (Saleh & Poza) for single tone measurements is determined by plotting the nonlinearity curves for both. The model for which the consistency in shape is more will be more accurate [10]. The larger question of which model is better for general inputs is unclear.

As pointed out by Blum [10] the model proposed by Abuelma'atti seems to be the best model yet for determining the IMPs and Harmonic amplitudes. The coefficients in Abuelma'atti's model can be obtained by approximating the input output instantaneous characteristics by a Fourier series method to desired accuracy.

We decided to implement the model proposed by Abuelma'atti [15]. The next step was to develop the experimental setup and supporting routines for determination and calculation of output at IMPs. Riley [16], has developed a prediction program that firstly, determines the frequencies of potentially problematic intermodulation products and secondly, evaluates their relative amplitudes. They have brought together two manual procedures to produce an efficient computer based model of intermodulation spectra. The first method is the graphical reduced frequency spectra generation scheme developed by Frank Box [17]. They have merged

it with a simple amplitude computation method [18] to calculate the output amplitudes. Abuelma'atti and Gardiner [18], used the first and third components of the Fourier series and a specified(fixed) nonlinearity to calculate simple IMP amplitude levels. Riley's implementation does not include a facility to automatically determine the characteristics and its approximation. They take the Fourier series coefficients and then predict IMP amplitudes.

In order to determine the output amplitudes at IMPs and Harmonics, we aim to take the following steps:

- A data acquisition system will be implemented to determine instantaneous characteristics of circuits.
- Abuelma'atti's frequency-dependent model will be simulated to determine the amplitude nonlinearities.
- An algorithm to determine the IMP frequencies will be developed.
- IMP amplitudes will be calculated and compared with experimental results.

In short, the aim of this volume is to present an implementation of a frequency dependent model. The implementation will be experimentally verified. Therefore the work will validate the frequency dependent model presented by Abuelma'atti [15]. This work will also serve as a prototype for a stand alone IMP prediction and correction system, the need for which has kept researchers involved in investigation of nonlinearities.

1.4 Thesis Contribution

This thesis will be the first attempt to implement a frequency dependent model. This work will validate the model proposed by Abuelma'atti. The circuits will be tested by multitone excitation and intermodulation behavior will be reported.

1.4.1 Implementation Process

In order to accomplish the objectives of the thesis, the following steps have been taken:

- A data acquisition system (DAS) has been designed, implemented, and calibrated by comparison with a commercial system.
- The limitations of the DAS have been discussed.
- A commercial data acquisition system has also been used to acquire data at frequencies beyond the capabilities of the designed DAS.
- A characteristic approximation technique has been implemented that readily calculates the coefficients required by the model.
- A user friendly software has been developed that achieves the following purposes :

  1. Controls the data acquisition system and records the amplifier's characteristics.
  2. Uses the recorded data and a Fourier-series method to approximate the characteristics and generats coefficients. The number of coefficients generated is be controlled by the user defined accuracy.
  3. Calculates the frequency dependent and independent parameters of the model using previously generated coefficients.
  4. Prompts the user to input ampitudes and frequencies involved in the multitone signal. The user also inputs the order of the desired intermodulation products.
  5. Depending on the defined order of IMPs, determines the frequencies and calculates the corresponding output amplitudes.

- The output spectrum of the circuits has been experimentally recorded using a spectrum analyser.
- The results calculated by the model have been compared with the experimental results and errors have been reported.
- Practical limitations have been discussed and suggestions for future work are outlined.

1.5 Thesis Organization

The thesis work is presented as follows:

- Chapter 1 gives a brief introduction to IMP's generated by nonlinearities of electronic devices and defines the thesis objectives. In addition, a detailed literature review of different proposed models is also given.
- Chapter 2 outlines in detail the frequency dependent model, the approximation technique, and other supporting algorithms used in the thesis work.
- Chapter 3 is devoted to the hardware implementation of the DAS. Complete designs of different parts of the hardware are discussed in detail alongwith their limitations. A commercial system used in the implementation is also discussed.
- Chapter 4 contains the circuits which have been tested by our implementation system and results are discussed.
- Chapter 5 concludes the thesis by outlining suggestions for future work.

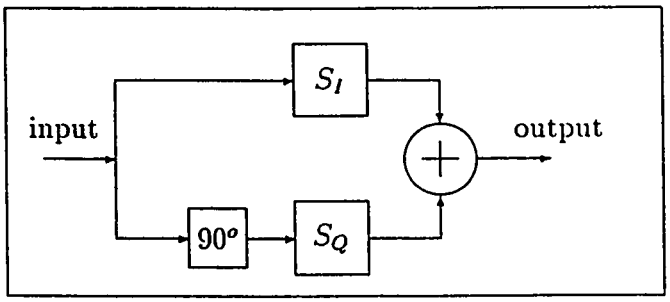

Figure 1.3: Quadrature Model of TWT

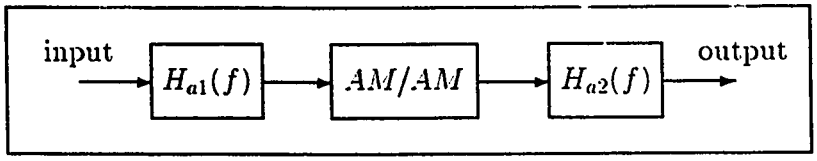

Figure 1.4: Construction of Frequency Dependent AM/AM Block

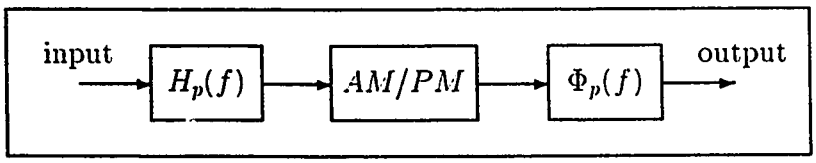

Figure 1.5: Construction of Frequency Dependent AM/PM Block

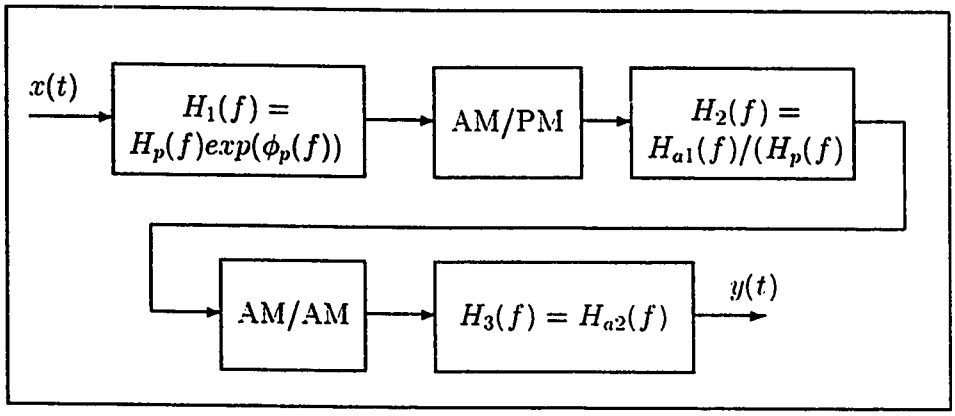

Figure 1.6: Poza's Serial Block Structure for Frequency Dependent TWT Model
x(t) : Input & y(t) : Output

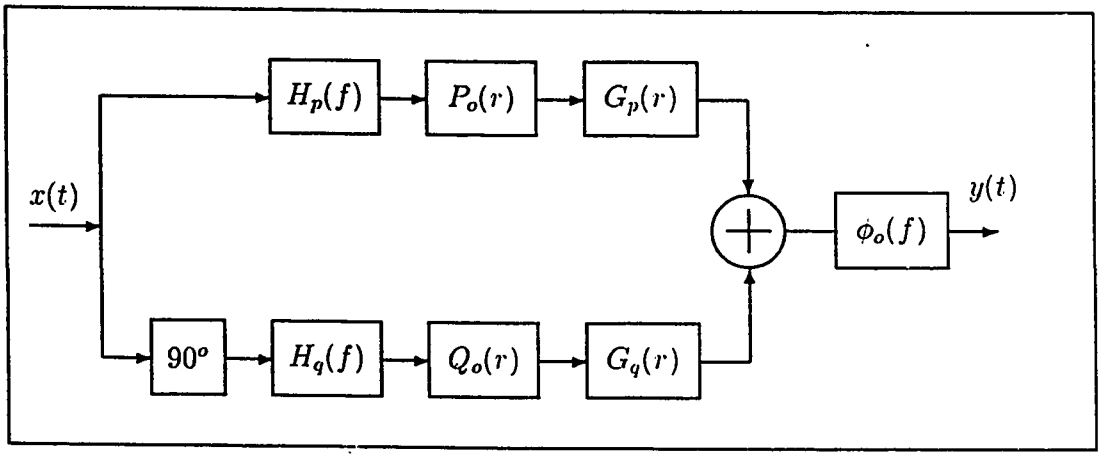

Figure 1.7: Implementation of Saleh's Model
$x(t)$: Input $y(t)$ = Output

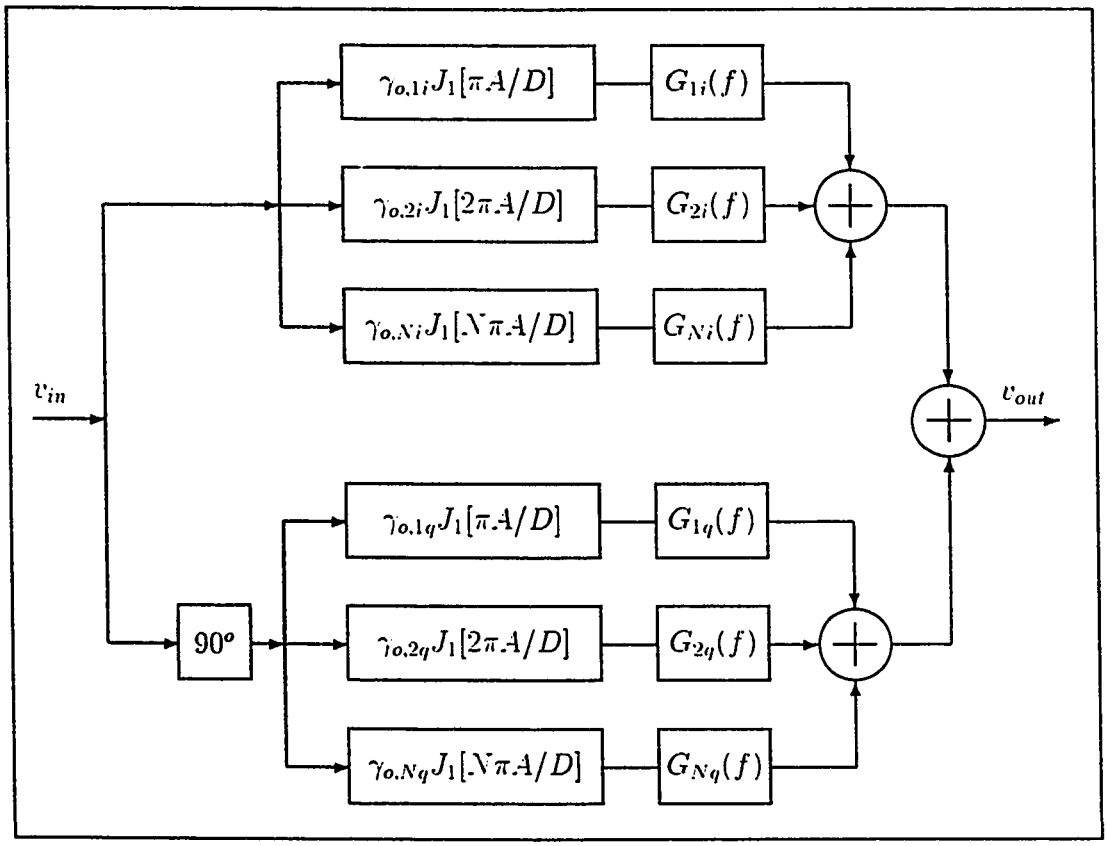

Figure 1.8: Abuelma'atti Frequency Dependent Model

Chapter 2

Device Models & Algorithms

2.1 Introduction

An integrated system to determine the output amplitudes of the Intermodulation Products (IMP) and Harmonics would have to incorporate:

- Device under test.
- A facility to acquire data characterizing the test device.
- A characteristic approximation facility.
- A model to simulate the device behavior.
- Algorithms to calculate the IMP frequencies and their amplitudes.
- Supporting routines for mathematical functions used in model.

The design and implementation of the Data Acquisition System (DAS) will be discussed in detail in the next chapter. As pointed out in the last chapter, the model proposed by Abuelma'atti [15] is considered to be the best model yet due to the fact that it does not assume any curves to maintain their shape from one frequency to another. In order to implement the model it is necessary to approximate

the characteristics. This should be done in a manner so that the generated approximation coefficients can be easily incorporated in further calculations. The model uses Bessel functions to approximate the nonlinearities hence a routine to calculate them should also be incorporated. In the following sections Abuelma'atti's model and different algorithms used for complete implementation of frequency dependent model are discussed.

2.2 Abuelma'atti's Model

It is frequently valuable in the design of electronic circuits to have a rapid indication of the likely spectrum of output signals, including intermodulation products, from a nonlinear componenet of the system whose characteristics are known from published data sheets, gain measurements, or from the instantaneous characteristics. A widely used procedure involves derivation of a high order polynomial approximation to the instantaneous device characteristics. Abuelma'atti [15] proposed a frequency independent quadrature model for a Travelling Wave Tube (TWT) and extended the concept to incorporate the frequency dependency of TWT. The same concept is applicable to devices having saturating instantaneous characteristics.

2.2.1 Frequency Independent Quadrature Model

If the the input signal to a nonlinear device, represented by the quadrature model of Fig. 2.1, is

$$x(t) = A\cos(2\pi f_o t + \sigma_o) \tag{2.1}$$

where A is the input peak amplitude, f_o the input signal frequency, and σ_o is the associated phase. The nonlinearities of the device will result in a signal at the output whose amplitude and phase are a function of the inpit amplitude

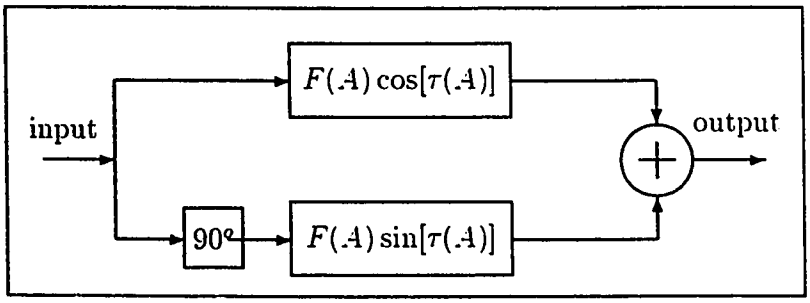

Figure 2.1: Quadrature Frequency Dependent Model

$$\begin{aligned} IIIY(t) &= F(A)\cos(2\pi f_o t + \sigma_o + \tau(A)) \\ &= F(A)\cos(2\pi f_o t + \sigma_o)\cos(\tau(A)) - \\ &= F(A)\sin(2\pi f_o t + \sigma_o)\sin(\tau(A)) \end{aligned}$$

the output is given by the sum of the inphase and quadrature components, as

$$Y_I(t) = F(A)\cos[\tau(A)]\cos(2\pi f_o + \sigma_o) \tag{2.2}$$

$$Y_Q(t) = F(A)\sin[\tau(A)]\cos(2\pi f_o + \sigma_o) \tag{2.3}$$

where $F(A)\cos[\tau(A)]$ and $F(A)\sin[\tau(A)]$ are the inphase and quadrature nonlinearities determined from the measured frequency independent amplitude nonlinearity $F(A)$ and the AM/PM conversion, $\tau(A)$, characteristics of the device.

The inphase and quadrature nonlinearities are represented by the sum of Bessel functions of the form

$$F(A)\cos[\tau(A)] = \sum_{n=1}^{N} \gamma_{nI} J_1\left(\frac{n\pi A}{D}\right) \tag{2.4}$$

$$F(A)\sin[\tau(A)] = \sum_{n=1}^{N} \gamma_{nQ} J_1\left(\frac{n\pi A}{D}\right) \tag{2.5}$$

where $J_1(.)$ is the Bessel function of the first kind of order one, 2D is the dynamic range of the input voltage measured in volts, and $\gamma_{nI(Q)}$ are fitting parameters which can be obtained using a minimum mean square error or relative root mean square error (RRMS) curve fitting procedure to fit equations 2.4 and 2.5.

By using the representations of 2.4 and 2.5, the amplitude $V_{(\alpha_1,\alpha_2,....,\alpha_M)}$ of an output product of frequency

$$\sum_{m=1}^{M} \alpha_m f_m$$

resulting from exciting the device by a multitone input signal of the form

$$\sum_{m=1}^{M} V_m \cos 2\pi f_m t \tag{2.6}$$

is calculated by [19] as

$$V_{(\alpha_1,\alpha_2,....,\alpha_M)I(Q)} = \left[(V_{(\alpha_1,\alpha_2,....,\alpha_M)I})^2 + (V_{(\alpha_1,\alpha_2,....,\alpha_M)Q})^2\right]^{1/2} \tag{2.7}$$

$$V_{(\alpha_1,\alpha_2,....,\alpha_M)I(Q)} = \sum_{n=1}^{N} \gamma_{nI(Q)} \prod_{i=1}^{M} J_{|\alpha_i|}\left(\frac{n\pi V_i}{D}\right) \tag{2.8}$$

here α_m is a positive or negative integer or zero, $J_{|\alpha_i|}(.)$ is the Bessel function of the first kind of order $|\alpha_i|$, and $\sum_{m=1}^{M} |\alpha_m|$ is the order of the output product and is an odd integer.

2.2.2 Frequency Dependent Quadrature Model

A device exhibiting frequency dependent amplitude nonlinearity (AM/AM) as well as phase nonlinearity (AM/PM conversion) will have a different pair of characteristics for each input frequency 'f'. Using the Relative Root Mean Square (RRMS)

curve fitting procedure, a model is derived for each input frequency. This would result in the frequency dependent parameters $\gamma_{nI}(f)$, and $\gamma_{nQ}(f)$, $n = 1 \rightarrow N$. Using the RRMS curve fitting procedure, these frequency dependent parameters can be approximated closely by

$$\gamma_{nI(Q)}(f) = \gamma_{on_{I(Q)}} G_{n_{I(Q)}}(f), \quad n = 1 \rightarrow N \tag{2.9}$$

where $\gamma_{on_{I(Q)}}$ are frequency independent parameters, and $G_{n_{I(Q)}}(f)$ are functions of frequency f.

Using equation (2.8), the frequency independent model of Fig. 2.1 is modified to accomodate the frequency dependence of the parameters $\gamma_{n_{I(Q)}}$ given by equation (2.9). This results in the frequency dependent quadrature model of Fig. 2.2. In each branch the input signal first passes through the frequency independent envelope nonlinearity

$$\gamma_{on_{I(Q)}} J_1 \left(\frac{n\pi A}{D}\right)$$

and then the output amplitudes are scaled by the filter $G_{n_{I(Q)}}(f)$.

Therefore, a multitone input signal with arbitrary tone amplitudes of the form in equation 2.6 are processed by several parallel connected branches. Each branch consists of a frequency independent amplitude nonlinearity followed by an appropriate filter. For example, at the output of the frequency independent nonlinearity

$$\gamma_{on_{I(Q)}} J_1 \left(\frac{n\pi A}{D}\right)$$

a wide range of products will be produced and, by using equation 2.8 the amplitude of the output product of frequency

$$\sum_{m=1}^{M} \alpha_m f_m$$

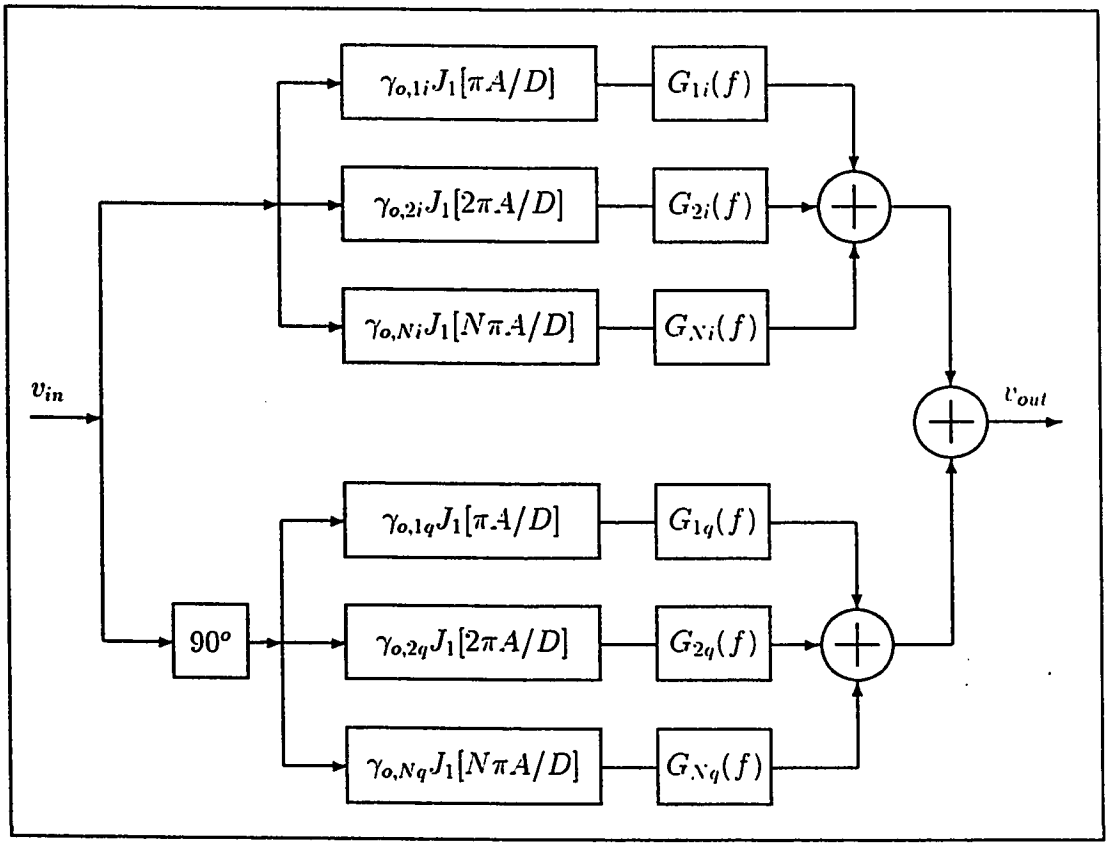

Figure 2.2: Frequency Dependent Quadrature Model

will be given by

$$\gamma_{on_{I(Q)}} \prod_{i=1}^{M} J_{|a_i|}\left(\frac{n\pi V_i}{D}\right).$$

Due to the filter action, this amount will be scaled by the amount

$$G_{n_{I(Q)}}\left(\sum_{m=1}^{M} a_m f_m\right)$$

before reaching the summing point, where the amplitudes of the output product of the same frequency will be summed up vectorially. Therefore, the amplitude of the output product of frequency

$$\sum_{m=1}^{M} a_m f_m$$

will be given by

$$V_{(a_1,a_2,\ldots,a_M)I(Q)} = \left[(V_{(a_1,a_2,\ldots,a_M)I})^2 + (V_{(a_1,a_2,\ldots,a_M)Q})^2\right]^{1/2} \tag{2.10}$$

where

$$V_{(a_1,a_2,\ldots,a_M)I(Q)} = \sum_{n=1}^{N}\left[\left(\gamma_{on_{I(Q)}} \prod_{i=1}^{M} J_{|a_i|}\left(\frac{n\pi V_i}{D}\right)\right) G_{n_{I(Q)}}\left(\sum_{m=1}^{M} a_m f_m\right)\right] \tag{2.11}$$

Equations 2.8 and 2.11 are similar with $\gamma_{n_{I(Q)}}$ replaced by

$$\gamma_{on_{I(Q)}} G_{n_{I(Q)}}\left(\sum_{m=1}^{M} a_m f_m\right) \tag{2.12}$$

Abuelma'atti applied the model to TWT characteristics and used exponential functions to approximate the frequency dependent coefficients. In this work we have used Fourier series for characteristic approximation to generate frequency-independent coefficients. The same Fourier series approach is used to approximate the coefficients for the frequency-dependent model.

2.3 Fourier Series Approximation

At present many methods and criteria are available for fitting measured, or experimental data by well defined mathematical functions, such as, algebraic polynomials and Fourier series. With the use of real-time systems, the fitting of operational data by simple and readily computable functions is of great importance. In this regard Smith [20] proposed a general method for fitting data to an Nth order polynomial according to least square criterion. The advantage of this method occurs because it makes use of simplifications that arise if the sequence of intervals at which the data is sampled, although arbitrary, is employed on a regular basis. The use of Smith's method requires a number of tables which give the values of the constants needed for calculating the polynomial parameters. The construction of these tables depends on the order of the polynomial and the number of sampled data points. However, in cases where the sequence of intervals at which the data is sampled is not regular, the advantage of this method cannot be gained. Alternatively, a single valued periodic function, $f(x)$, that is continuous, except for a finite number of discontinuities, in an interval $-B \leq x \leq B$ and has a finite number of maxima and minima in this interval, may be represented over the complete period 2B, except at the discontinuities, by a convergent Fourier series, [21], of the form

$$f(x) = \delta_o + \sum_{m=1}^{\infty} \left[\delta_m \cos\left(\frac{m\pi\, x}{B}\right) + \gamma_m \sin\left(\frac{m\pi\, x}{B}\right) \right] \tag{2.13}$$

where

$$\delta_o = \frac{1}{2B}\int_{-B}^{B} f(x)dx \tag{2.14}$$

$$\delta_m = \frac{1}{B}\int_{-B}^{B} f(x)\cos\left(\frac{m\pi x}{B}\right)dx \tag{2.15}$$

$$\gamma_m = \frac{1}{B}\int_{-B}^{B} f(x)\sin\left(\frac{m\pi x}{B}\right)dx \tag{2.16}$$

However, for odd functions with $f(x) = -f(-x)$, the coefficients $\delta_o = \delta_m = 0$,

and equation (2.13) reduces to

$$f(x) = \sum_{m=1}^{\infty} \gamma_m \sin\left(\frac{m\pi\, x}{B}\right) \tag{2.17}$$

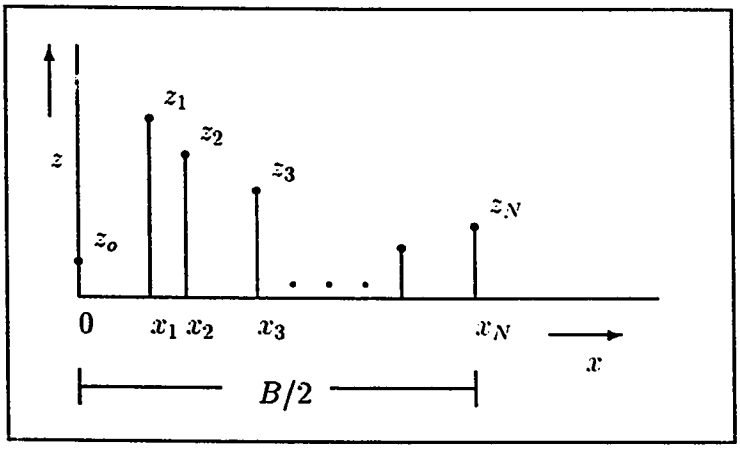

Figure 2.3: Data set z_n measured at x_n

In the general case, $f(x)$ will not be known in the functional form, but in the form of a set of say, $(N+1)$ points , z_n $n = 0, 1, ..., N$, measured at x_n $n = 0, 1, ..., N$ where $x_o = 0$ and $x_N = B/2$, as shown in Fig. 2.3. This set of data points represents measured samples of $f(x)$ in a duration B/2.

To make this set of points periodic with odd symmetry, first the offset at $x_o = 0$ has to be removed, and second the set of data has to be utilized in mirror imaging to generate a complete half period as shown in Fig. 2.4.

The parameters γ_m of the odd function $f(x)$, which includes the data points (x_n, y_n) such that $y_n = f(x_n)$, or the error

$$\sum_{n=1}^{N+1} (y_n - f(x_n))^2$$

is small, can be obtained using the standard curve fitting techniques or discrete Fourier-transform (DFT) techniques. These techniques invariably demand extensive

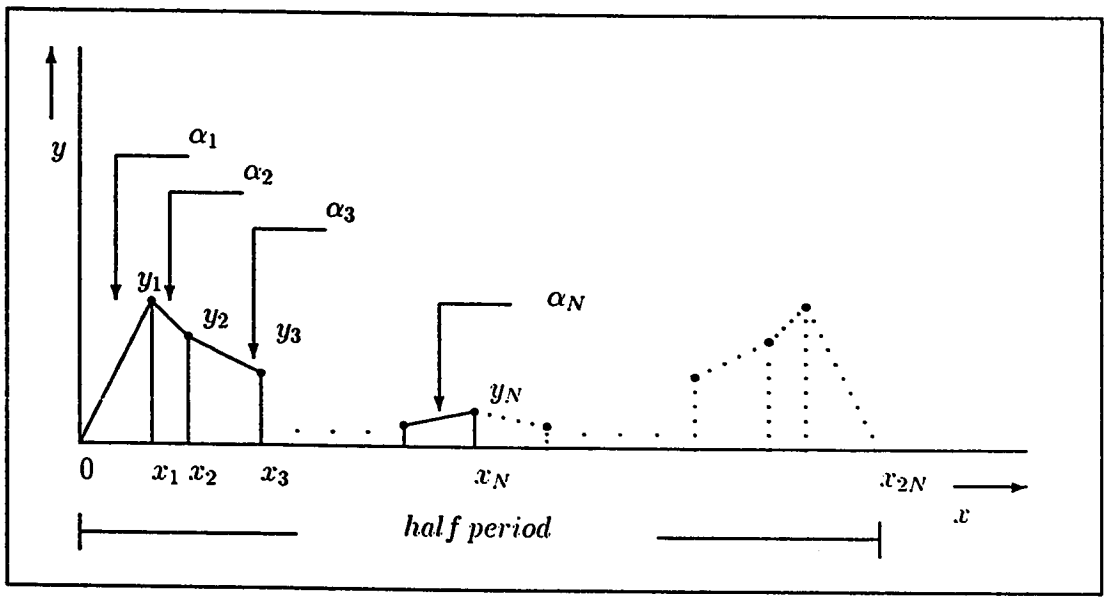

Figure 2.4: Data Set After Removing the Offset y_o, Imaging And Interpolation

computing facilities and well developed software. Moreover, to reduce the number of multiplications and additions involved in the DFT of a large number of equally spaced data, it is essential to organize the problem so that the number of data points can be easily factored, particular, in powers of two [22].

Alternatively, by using short cut methods [23, 24], the parameters γ_m can be obtained without the recourse to the DFT or standard curve fitting routines. Obviously, these methods are more appropriate for small dedicated microprocessor based systems. However, these methods are applicable only for even number of data points sampled at equally spaced sequences of intervals. Also, the resulting Fourier series has finite number of terms. The order of Fourier series is another important parameter as it effects the accuracy of resulting approximation. In general, a high order Fourier series requires a proportionally large number of sampled data points input for the short cut methods as well as the DFT and standard curve fitting techniques.

The algorithm proposed by Abuelma'atti [25] presents an alternative method

for obtaining the parameters γ_m. In principal the method is a short cut method. However, its advantages over the remaining short cut methods are:

- The feasibility of obtaining an infinite order Fourier series model using finite number of data points.
- The sequence of intervals at which the data is sampled is arbitrary and is not necessarily equally spaced. Also the number of data points is not necessarily even.

Moreover, in contrast with Smith's method the advantages of the proposed method can be gained whether the sequences at which the data is sampled are employed on regular or irregular basis.

2.3.1 Abuelma'atti's Fourier Series Method

In the general case, the function $f(x)$ of equation (2.16) will be available in the form of discrete number of data points. As a result the function $f(x)$ is interpolated between the measured data points by using $4N$ straight line segments joined end to end as shown in Fig. 2.4. The x-value of the segment joints are termed as knots. The number of knots and their positions must generally be chosen so that closer knots are placed in regions where the function $f(x)$ is changing rapidly. The knots are not necessarily equally spaced. By denoting the slope of each segment by α_n , as shown in Fig. 2.4, it is easy , following the procedure described by Kreyzig [26], to show, without performing the integration of equation (2.16), that the Fourier series coefficients γ_n are given by

$$\gamma_m = \frac{8x_N}{(m\pi)^2}\left[\alpha_N \sin\left(\frac{m\pi}{2}\right) + \sum_{n=1}^{N-1}(\alpha_n - \alpha_{n+1})\sin\left(\frac{m\pi}{2}\frac{x_n}{x_N}\right)\right] \quad m = odd \quad (2.18)$$

$$\gamma_m = 0 \quad m = even \quad (2.19)$$

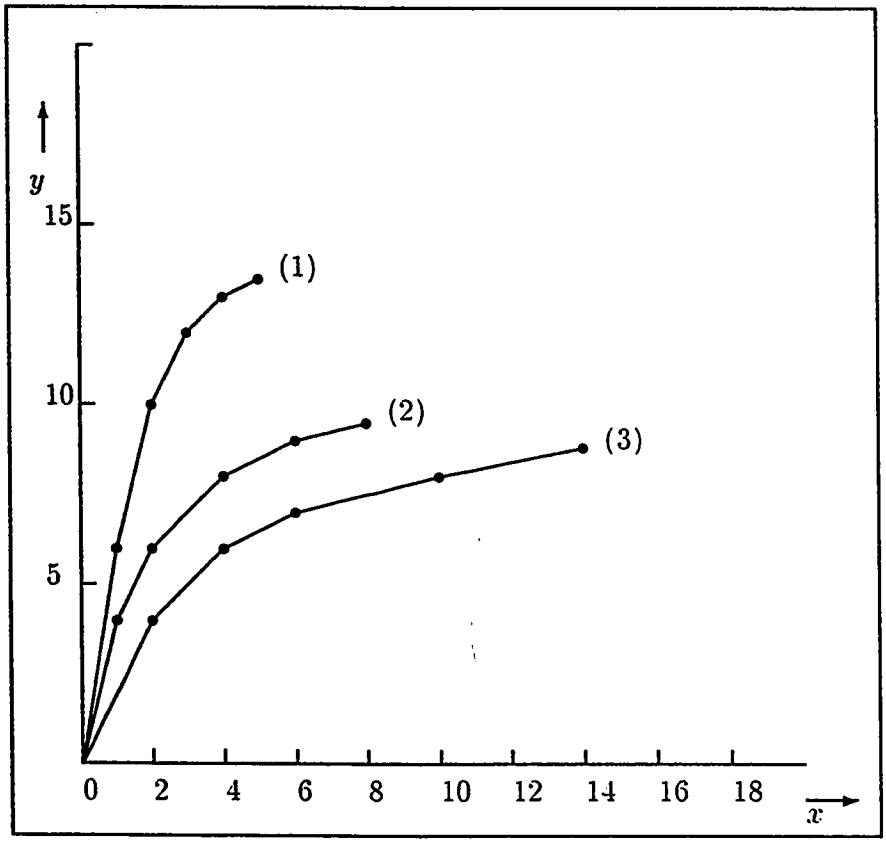

Figure 2.5: Data Sets Used to Investigate the Accuracy of Approach

From equation (2.18) it is obvious, [25], that, in contrast with DFT and curve fitting routines, calculation of γ_m for any value of 'm' requires only simple mathematical operations. Also, inspection of equation (2.18) suggests that as m becomes large, the Fourier-series coefficients γ_m approach zero.

Using equation (2.18), any set of measured data points, at any sequence of interval, can be fitted to a Fourier series model to any degree of accuracy by using as many terms as necessary. The number of γ_m terms is allowed to increase until the the desired accuracy in terms of Relative Root Mean Square Error (RRMS) is achieved. To investigate the accuracy of the algorithm for calculating γ_m the mea-

Data set	Terms	RRMS Error
(1)	10	0.14
(1)	20	0.05
(1)	50	0.03
(1)	70	0.026
(1)	100	0.020
(2)	10	0.13
(2)	30	0.046
(2)	50	0.029
(2)	70	0.022
(2)	100	0.016
(3)	10	0.141
(3)	30	0.048
(3)	50	0.030
(3)	70	0.022
(3)	90	0.017
(3)	100	0.016

Table 2.1: Effect of number of terms on Fourier series Technique

sured data points of Fig. 2.5 were fitted to the Fourier series model. Table (2.1) summarizes the results obtained for different number of coefficients of the Fourier series approximation.

2.3.2 Discussion

The use of Fourier series for representing measured or experimental data is bound to be fraught with Gibbs oscillation [27]. However, what is true for the Fourier series is clearly true for any other series representation. In most cases, the most satisfying fit is obtained by a series of appropriate number of terms, compromising between goodness of fit and the smoothness of the curve. Although no completely general rule can be given, Maron [28] recommends that in order to smooth error in the data, the number of data points should be greater than the order of the polynomial by at least four. Moreover, the fit will not necessarily improve by increasing the degree

of the polynomial. Increasing the degree allows the curve to wiggle more in order to come closer to the data. The least square error criterion ensures good fit for y_n near an original data point x_n , but in between successive x_n the fitted curve may oscillate. As the degree of the polynomial increases, the mean square error is reduced, yet the oscillations increase [29].

The Fourier series representation required extending the measured or experimental data in order to be periodic. This raises a question of how to periodically extend the data. Two possibilities exsist and are illustrated in Fig. 2.6a, and 2.6b. In the first method, shown in Fig. 2.6a, the final value of the data is forced to be equal to the starting value, via a discontinuity, before mirror imaging to form a complete period. The resulting Fourier series will, therefore, be formed of odd order sine functions. In the second method, shown in Fig. 2.6b, the final value of the data is forced to equal to the starting value in a physical manner by mirror imaging to form a complete half period and then the half period data is mirror imaged to form a complete period.

The disadvantage of the first method is that by making the period equal to $2x_N$, all terms in sine series will have zero crossing at x_N. The resulting curve, therefore, diverges substantially from the measured data near x_n. The resulting ringing is the result of Gibbs phenomenon [27]. Taking more terms in the Fourier series does not reduce the magnitude of the overshoot, all it does is to compress it along the x-axis in the vicinity of the discontinuity at $x = x_n$ [29]. By making the period larger than $2x_n$, the largest oscillations can be moved away from the part of the curve over which an accurate representation is required [30]. However, by using the second method, which is adopted in the algorithm by Abuelma'atti [25], the Gibbs phenomenon is totally avoided especially if the measured or experimental data does not contain any discontinuities, as is usually the case encountered in most practical devices and systems. It is worthwhile mentioning here that removing the offset z_o at $x = x_o$, in

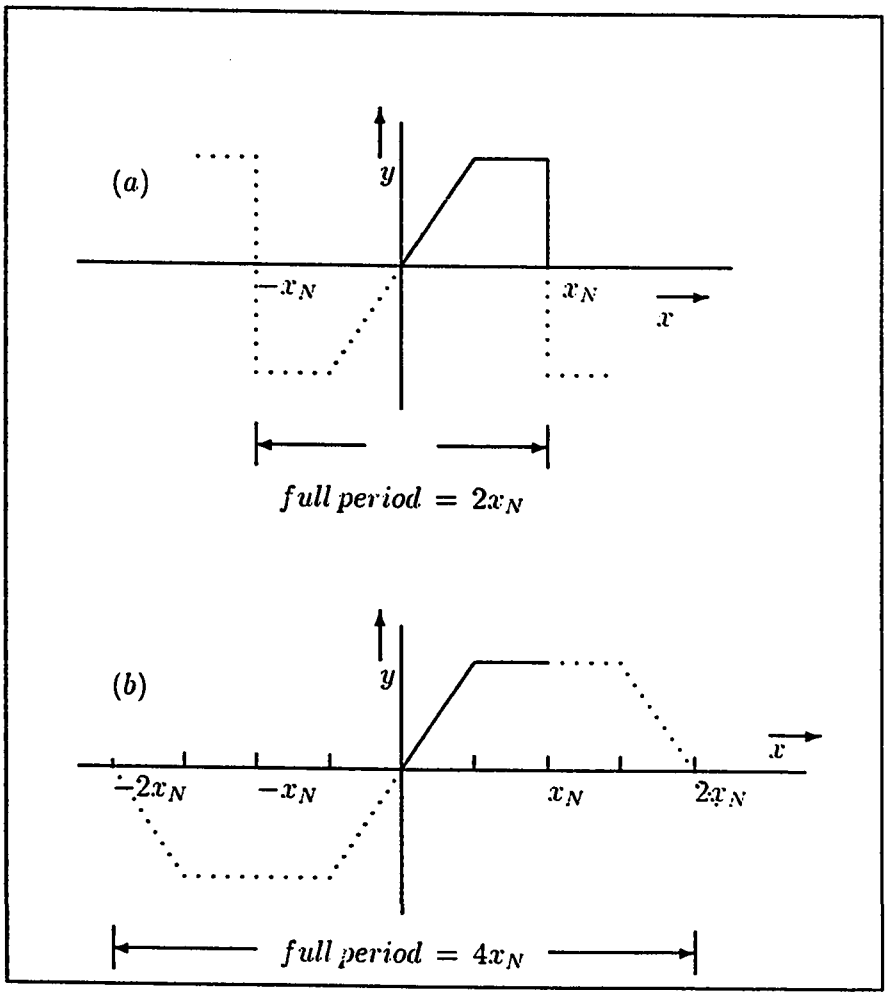

Figure 2.6: Extension of Measured Data

order to periodically extend the data can be easily corrected by adding the offset to the resulting Fourier series. Finally, although the algorithm can produce an infinite order Fourier series, in most practical cases the series must be truncated after a finite number of terms.

2.4 Bessel Function Calculation

In the sine series model, Abuelma'atti's model, the frequency independent nonlinearities are expanded in the terms of first order Bessel functions. The amplitude $V_{(\alpha_1,\alpha_2,....,\alpha_M)}$ of an output product of frequency

$$f_{result} = \sum_{m=1}^{M} \alpha_m f_m \tag{2.20}$$

where f_{result} is the resulting IMP, M is the total number of input signals, α_i is an integer, and f_m is the frequency of the input signal, resulting from exciting the device by a multitone input signal is calculated, as

$$V_{(\alpha_1,\alpha_2,....,\alpha_M)I(Q)} = \left[(V_{(\alpha_1,\alpha_2,....,\alpha_M)I})^2 + (V_{(\alpha_1,\alpha_2,....,\alpha_M)Q})^2\right]^{1/2} \tag{2.21}$$

$$V_{(\alpha_1,\alpha_2,....,\alpha_M)I(Q)} = \sum_{n=1}^{N} \gamma_{nI(Q)} \prod_{i=1}^{M} J_{|\alpha_i|}\left(\frac{n\pi V_i}{D}\right) \tag{2.22}$$

Here α_m is a positive or negative integer or zero and $J_{|\alpha_i|}(.)$ is the Bessel function of the first kind of order $|\alpha_i|$, and $\sum_{m=1}^{M} |\alpha_m|$ is the order of the output product and is an odd integer.

It is obvious from above discussion that Bessel function of different orders are required, the argument of which would be decided by the input amplitudes, number of coefficients and the Dynamic range. We must have some means of computing the Bessel functions, since it is impractical to store the values reported in mathematical handbooks Waldron [31] have obtained formulas for $J_o(x)$ and $J_1(x)$ in terms of trigonometric functions as:

$$J_o(x) = \frac{1}{4}\left[1 + \cos x + 2\cos(x/\sqrt{2})\right] \tag{2.23}$$

$$J_1(x) = \frac{1}{4}\left[\sin x + \sqrt{2}\sin(x/\sqrt{2})\right] \tag{2.24}$$

The equations 2.23 and 2.24 are applicable for values of $x \leq 3$. Higher order Bessel functions can be obtained by using the recurrence relation

$$J_{n-1}(x) + J_{n+1} = \frac{2n}{x}J_n(x) \tag{2.25}$$

For values of $x \geq 3 \leq \infty$ the values of $J_o(x)$ and $J_1(x)$ are computed by the formulae given in *Handbook of Mathematical Functions* [32] as :

$$J_o(x) = x^{1/2} f_o \cos\theta_o \tag{2.26}$$

here

$$\begin{aligned} f_o &= 0.79788456 - 0.0000077(3/x) \\ &\quad - 0.00552740(3/x)^2 - 0.00009512(3/x)^3 \\ &\quad + 0.00137237(3/x)^4 - 0.00072805(3/x)^5 \\ &\quad + 0.000144476(3/x)^6 + \epsilon \end{aligned} \tag{2.27}$$

with $|\epsilon| < 1.6 \times 10^{-8}$ and

$$\begin{aligned} \theta_o &= x - 0.78539816 - 0.04166397(3/x) \\ &\quad - 0.00003954(3/x)^2 + 0.00262573(3/x)^3 \\ &\quad - 0.00054125(3/x)^4 - 0.00029333(3/x)^5 \\ &\quad + 0.00013558(3/x)^6 + \epsilon \end{aligned} \tag{2.28}$$

with $|\epsilon| < 7 \times 10^{-8}$.

$$J_1(x) = x^{-1/2} f_1 \cos\theta_1 \tag{2.29}$$

where

$$\begin{aligned} f_1 &= 0.79788456 + 0.00000156(3/x) \\ &\quad + 0.01659667(3/x)^2 + 0.00017205(3/x)^3 \\ &\quad - 0.00249511(3/x)^4 + 0.00113653(3/x)^5 \\ &\quad - 0.00020033(3/x)^6 + \epsilon \end{aligned} \tag{2.30}$$

with $|\epsilon| < 4 \times 10^{-8}$ and

$$\begin{aligned} \theta_1 &= x - 2.35619449 + 0.12499612(3/x) \\ &\quad + 0.00005650(3/x)^2 - 0.00637879(3/x)^3 \\ &\quad + 0.00074348(3/x)^4 + 0.00079824(3/x)^5 \\ &\quad - 0.00029166(3/x)^6 + \epsilon \end{aligned} \tag{2.31}$$

with $|\epsilon| < 9 \times 10^{-8}$.

The equations have been implemented by a software routine, using the bounds for error ϵ as specified in the handbook [32]. The argument and its value are pseed to the routine and corresponding formulae are used for computation of $J_o(x)$ and $J_1(x)$. Higher order Bessel functions are computed by the recurrence formula.

2.5 Computation of IMP Frequencies

Harmonics and intermodulation products (IMPs) are generated when two or more frequencies are applied simultaneously to a device having nonlinear characteristics. For example, the application of three frequencies f_1, f_2, f_3 simultaneously to a device whose characteristics are given by the third order polynomial:

$$y = ax + bx^2 + cx^3 \tag{2.32}$$

gives rise to a spectrum consisting of up to 32 frequencies between DC and sum of the input frequencies. The maximum order of IMP in this case would be 3 because the characteristics are being approximated by a polynomial of degree 3.

The frequency of the IMP is computed by

$$f_{IMP} = \sum_{m=1}^{M} \alpha_m f_m \tag{2.33}$$

here f_{IMP} is the resulting IMP, M is the total number of input signals, f_m is the frequency of input signals and α_m are the corresponding weights. Order of the IMP is calculated as

$$Order = \sum_{m=1}^{M} |\alpha_m| \tag{2.34}$$

In case of sine series approximation there is no restriction on the order of the IMP and we must have means for computing the IMPs of any order for any number of input signals. We have developed a routine that takes as input the number of signals and order of the IMPs desired and generates all the possible frequencies. Since the characteristics have been monitored over a limited band of frequencies, the IMPs lying outside that band are automatically rejected.

2.6 Integration of Routines

The Frequency Dependent Model, Fourier-series approximation, Intermodulation Product generation and output computation have been explained in the previous sections. We have implemented the algorithms in *C language*.

Initially the device characteristics are approximated using Fourier-series approach to generate frequency independent fitting coefficients $\gamma_o m$. Here 'm' is the coefficient number and 'o' is the input signal number. The number of coefficients generated is dependent on the required accuracy. The coefficients for different input frequencies are again approximated using Fourier-series to generate frequency dependent coefficients. A generalized routine has been implemented to compute IMP

frequencies given number of signals and order. Using the equation (2.11) the output amplitudes for different frequencies are computed. A storage routine has been developed to store the IMP frequencies and corresponding amplitudes.

Chapter 3

Hardware Implementation

3.1 Introduction

In order to simulate any device it is necessary that information about its behaviour for different inputs is known. Most of the models characterizing electronic devices are based on their input-output characteristics. These characteristics can be amplitude or instantaneous input-output characteristics. Power series models can use both the characteristics since a clear relationship exsists between the coefficients generated by the amplitude and instantaneous approximation. The sine series approximation uses the instantaneous input-output relationship. It must be pointed out at this stage that it is not possible to use instantaneous characteristics when transit time devices (devices that introduce a time delay between input and output signals, e.g. Travelling Wave Tube) are used.

A complete data acquisition system (DAS) has been designed and implemented. The controlling software has been developed in *C language* with inline *Assembly language* commands to control the external circuitry. Block diagram of complete Hareware setup is represented in Fig. 3.1. System Hardware and software are discussed in the following sections.

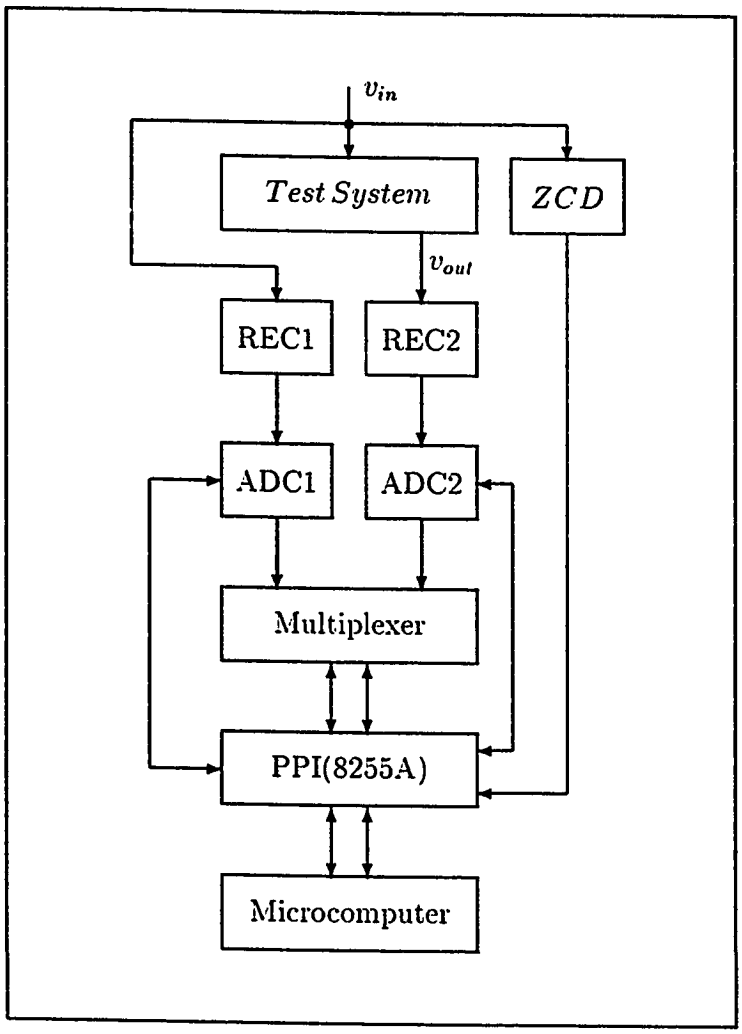

Figure 3.1: Block Diagram of Hardware Implementation
ZCD : Zero Crossing Detector, RECT1 : Input Rectifier,
RECT2 : Output Rectifier

3.2 Zero Crossing Detector

The zero crossing detector (ZCD) plays an important role in the data acquisition process. The data conversion is initiated by a rising edge (A Low-to-High transition) or a falling edge (A High-to-Low transition), depending on the programming options. The ZCD is implemented using two operational amplifiers, a switching diode and, a resistor. Fig. 3.2 shows the complete circuit diagram. The Op-amp (A1) is configured as a comparator with the positive input connected to the input sinusoidal signal and the negative input grounded. The output of Op-amp (A1), a bi-polar square wave of the same frequency as that of the input, is fed to a simple diode rectifier. The rectifier eliminates the negative half of the signal. The rectifier output is buffered to avoid loading. The input and output waveforms at different points in the circuit are depicted in Fig. 3.3 (for the purpose of demonstration triangular waveform are shown in figures).

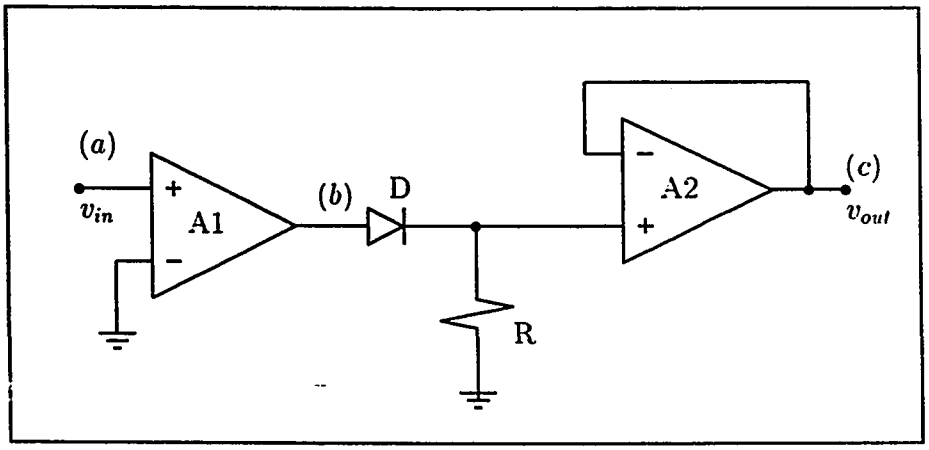

Figure 3.2: Zero Crossing Detector

Wide-band operational amplifiers and switching diodes are used to enable the circuit to operate at high frequencies. The operation of the circuit was practically verified from low frequencies up to 50kHz. Although a diode voltage drop would

be introduced at the rectifier output, the level is still recognized as low-level by the microprecessor.

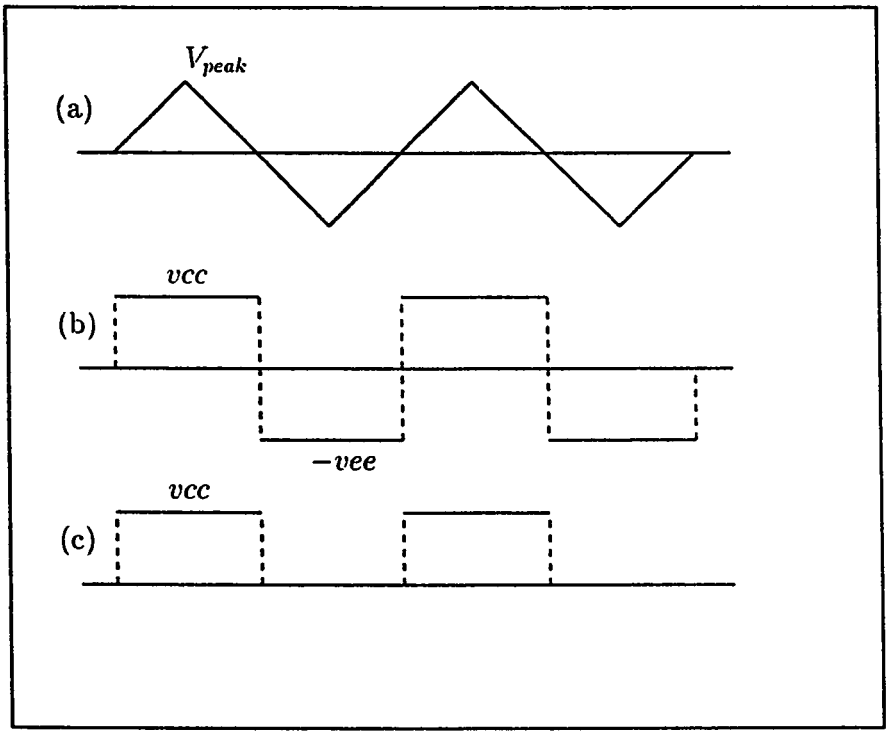

Figure 3.3: Input-Output of ZCD

3.3 Precision Rectifier Circuit

The input and output of the test circuits will be sinusoids having positive as well negative cycles and this would require configuring the ADC in bi-polar mode, reducing the ADC resolution. Therefore we have designed rectifiers for both input and output to ensure good resolution.

In the normal rectifier circuits the exact value of the diode drop is unimportant to the operation of the rectifier. Due to the fact that we are interested in exact values of the input and output signals it is important not to introduce the diode

drop at the output of rectifier. The circuit shown in Fig. 3.4 is the precision rectifier implemented.

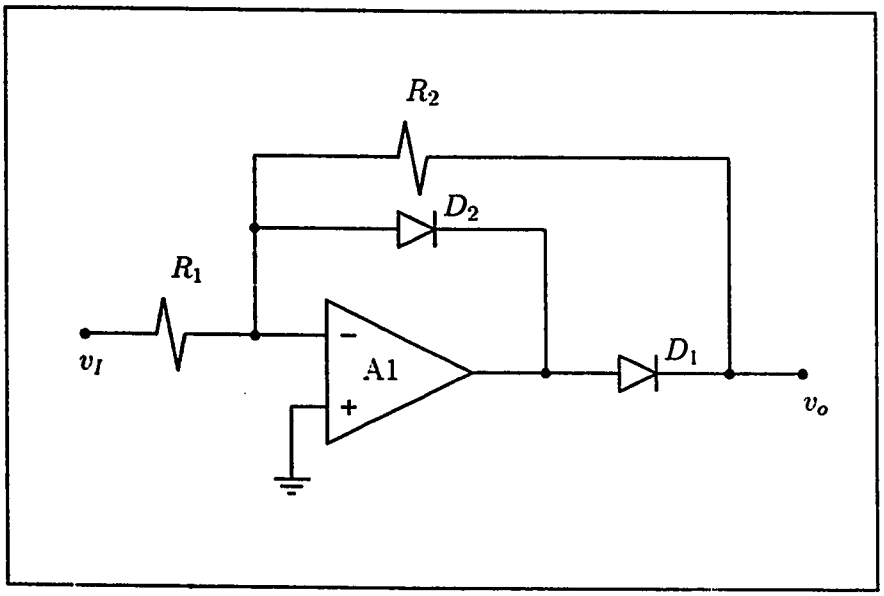

Figure 3.4: Percision Rectifier Circuit

The circuit operates in the following manner [33] : For positive voltage v_1 , diode D_2 conducts and closes the negative-feedback loop around the Op-amp. A virtual ground therefore will appear at the inverting input terminal, and the Op-amp's output will be clamped at one diode drop below ground. This negative voltage will keep diode D_1 off, and no current will flow in the feeback resistence R_2. It follows that the rectifier output voltage will be zero. As v_1 goes negative, the voltage at the inverting terminal will tend to go negative, causing the voltage at the Op-amp's output terminal to go positive. This will cause diode D_2 to be reverse biased and hence cut-off. Diode D_1, however, will conduct through R_2, thus establishing a negative-feedback path around the Op-amp and forcing a virtual ground at the inverting input terminal. The current through the feedback resistance R_2 will be equal to the current through input resistance R_1. Thus for $R_1 = R_2$ the output

voltage v_o will be

$$v_o = -v_I \ , v_I \leq 0 \tag{3.1}$$

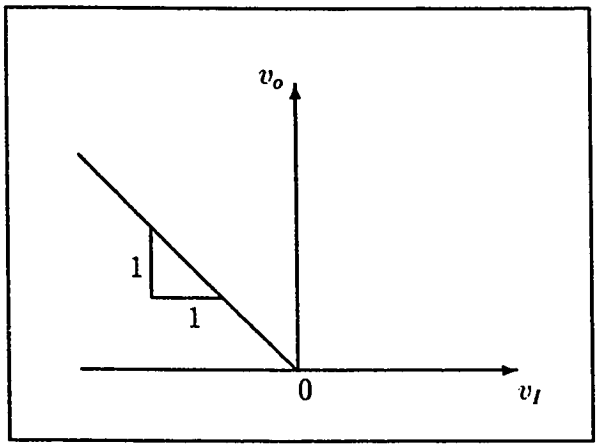

Figure 3.5: Transfer Characteristics of Percision Rectifier Circuit

The transfer characteristics of the circuit is shown in Fig. 3.5. The slope of the characteristics can be set to any desired value, including unity, by selecting appropriate values for R_1 and R_2. The major advantage of the circuit is that the feedback loop around the Op amp remains closed at all times. Hence the Op-amp remains in its linear operating region, avoiding the possibility of saturation and the associated time delay required to *get out* of saturation. Diode D_2 *catches* the output voltage as it goes negative and clamps it to one diode drop below ground, hence D_2 is called a *catching diode.* Again wide-band Op-amps and switching diodes are used to ensure proper operation over a wide-band of frequencies.

3.4 Analog to Digital Conversion

In order to obtain the instantaneous input-output characteristics of a device the analog signals must be converted into digital. This is achieved by using Analog

to Digital converters (ADC), triggered simultaneously by the microprocessor. The ADC's used are 12-bit successive approximation ADCs with a maximum conversion time of 36 micro seconds. They have 3-state output buffer circuitry for easy interfacing to microprocessor bus (8 or 16 bit). A high precision voltage reference and clock are included on-chip. The Read/Convert and Output enable signals are directly generated by the control bus of the microprocessor. However to facilitate the handshake signals, an additional Programmable Peripheral Interface chip has been used. The ADC has been externally configured to accomodate input voltages from 0V to +10V, resulting in a resolution of 2.44 mV.

A typical ADC converter interface involves several operations. A write to the ADC address initiates the conversion process. The processor must then wait for the conversion cycle to complete, since most ADCs take longer than one instruction cycle to complete the conversion. Valid data can, of course, be only read after the conversion is complete. The ADC used provides an output signal (STS) which indicates when a conversion is in progress. This signal is polled by the processor, reading it through an input port of Parallel Peripheral Interface (PPI). Once it is established that the conversion is complete the data can be read. Since the PPI has eight bit ports the data must be read in byte wide data format. A facility to achieve this is provided on the ADC , and the 12-bits of the output data are be read as two bytes (one with 8 data bits, other with 4 data bits and 4 trailing zeros).

3.5 Programmable Peripheral Interface

A Programmable Peripheral Interface (8255A) is a LSI peripheral designed to permit easy implementation of parallel I/O (Input/Output) in the microcomputer systems. It provides a flexible parallel interface, which includes features such as single-bit, 4-bit, and byte-wide inputs and output ports, level sensitive inputs, latched outputs, strobed inputs or outputs, and strobed bidirectional input/outputs. These features

are selected under software control [34].

The PPI includes an *8 bit bidirectional data bus* over which, commands, status information, and data are transferred between the microprocessor and the PPI. The PPI has four internal registers

- CONTROL Register
- PORTA Register
- PORTB Register
- PORTC Register.

All the registers have separate addresses hence, they can be treated as independent memory locations. The data from or to these registers is transferred whenever the microprocessor performs an input or output bus cycle to an address within the device, when configured as isolated I/O . Timing to the PPI is controlled by the *read/write* ($\overline{RD}$ *and* $\overline{WR}$) *control* signals.

3.6 Personal Computer Interface

The input/output (I/O) interface card designed for this implementation, shown in Fig. 3.6, is compatible with IBM PC-XT and IBM PC-AT systems. The card has been wired on a board which can be installed directly inside the computer. It can be added on to any of the expansion slots located on the mother board.

The I/O card is composed of a bidirectional buffer (B1) for the data lines. a unidirectional buffer (B2) for the control signals and two address lines and an eight bit magnitude comparator (C1) for address decoding. A DIP switch (D1) is also used to apply the required address to magnitude comparator.

The data lines $D0 - D7$ are buffered by the bidirectional 8-bit buffer to prevent loading of the data lines. The RESET line and the address lines $A0$ and $A1$ are

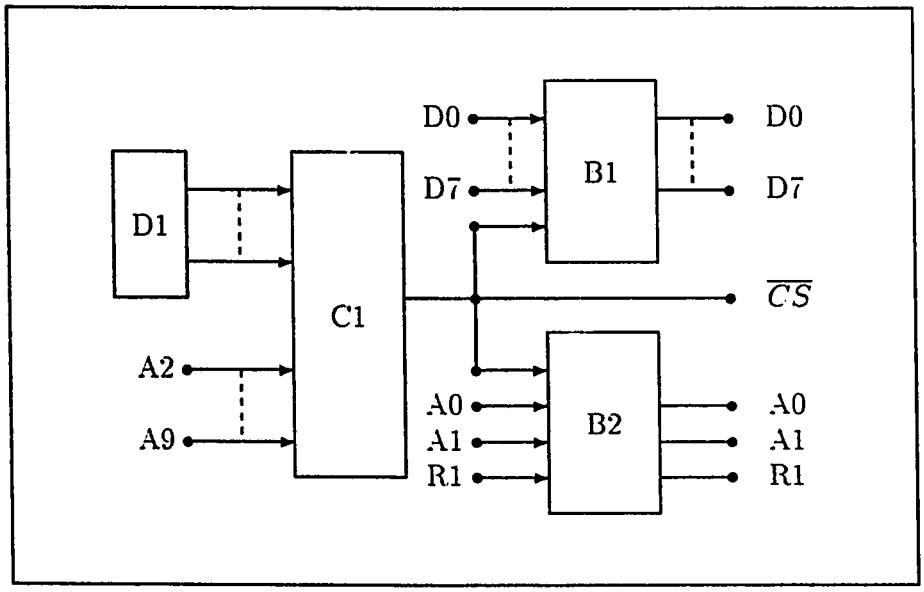

Figure 3.6: I/O Card circuit
R1 : RESET Signal, D1 : Dip Switch, C1 : Magnitude Comparator, B1 : Bidirectional Buffer, B2 : Unidirectional Buffer

buffered by the unidirectional buffer. The $\overline{RD}$ and $\overline{WR}$ control signals are buffered by using an AND gate.

The I/O card is decoded as Isolated I/O. The address decoding is done by comapring the address on the address lines $A9 - A2$ with that applied by the DIP SWITCH setting. An 8-bit magnitude comparator generates an active low signal when the input magnitudes are equal. The state of the address line under this condition would be

$$\begin{array}{cccccccccc} A9 & A8 & A7 & A6 & A5 & A4 & A3 & A2 & A1 & A0 \\ 1 & 1 & 0 & 0 & 0 & 0 & 0 & 0 & X & X \end{array} \tag{3.2}$$

The output signal from the magnitude comparator is used as the gating signal for the two buffers and as $\overline{CS}$ input to the subsequent 8255A PPI.

3.7 Circuit Operation

The circuit is controlled by a software package developed in *C language* with inline *Assembly language* instructions. The flow chart for the program is depicted in Fig. 3.7 and 3.8. Initially the PPI is configured, with PORTA and PORTB as input ports and PORTC as an output port. The outputs of the two ADC's are coupled to a digital multiplexer. The output from the multiplexer is connected to the PORTA of the PPI. PORTB of the PPI is an input port for the control signal from ZCD and conversion complete signals, STS1 and STS2, from the ADCs. The PORTC is an output port controlling the ADCs and the multiplexer.

Once the configuration is complete the user inputs the number of input frequencies over which the characteristics are to be obtained. The program would automatically determine the filenames for different frequencies. The user is prompted to connect the two ADCs to GND and $+5\,volts$ respectively for calibration and voltage conversion purposes.

After configuration and calibration a delay counter with an initial value of zero

and a routine to recognize ZCD is initiated, when a low to high transition is detected a begin conversion signal (Convert) is applied to both the ADCs. The program waits for the conversion completion by polling the STS signals from the ADCs. When the conversion is complete the 12-bit data from the two ADCs is read in 8-bit formats and stored in corresponding arrays. The data flow is controlled by the output enable and multiplexer select signals. The delay counter is then incremented and the whole process is repeated until a decrease in input signal level is detected.

3.8 Limitations of the Circuit

The circuit was calibrated by comparing the results with those from a commercial data acquisition system. The circuit operated efficiently uptill 5kHz but any attempt to go beyond this freqeuncy resulted in significant errors in the obtained values. This limitation can be attributed to the following :

- Time is lost in storing data in arrays.
- Polling of status signals and decision making requires time.
- The PPI has level sensitive inputs.

3.9 Implementation on Commercial system

The data acquisition system (DAS) designed was unable to operate on frequencies higher than 5KHz. In order to validate the model it was necessary that results obtained be verified experimantally. This requires exciting the test system by a multitone signal and observing the output on a spectrum analyzer. The spectrum analyzer available did not operate properly at low frequencies. Hence it was necessary to increase frequency of data acquisition. A NI-DAQ commercial data acquisition board, AT-MIO-16L, has been used to acquire data (input/output characteristics).

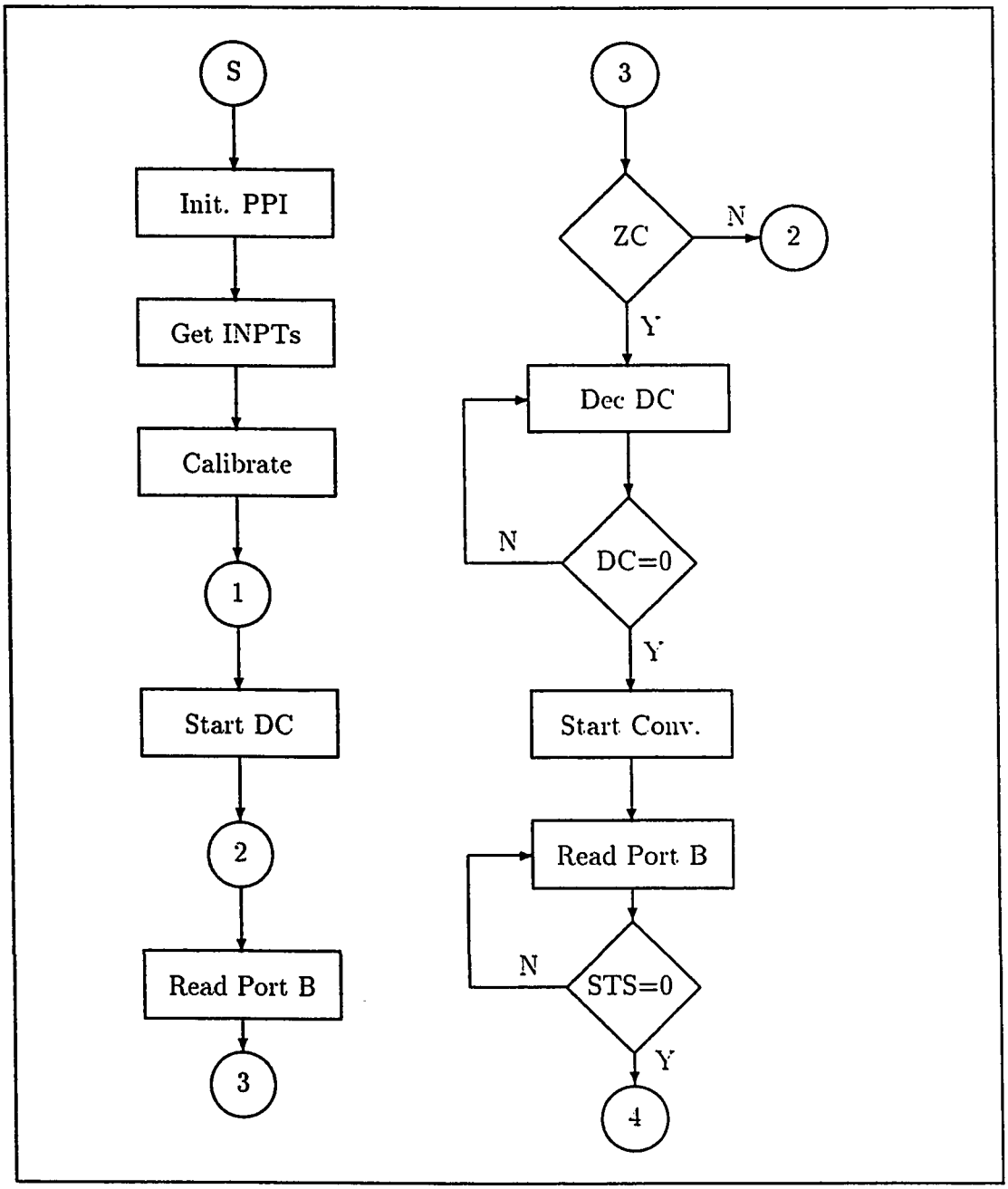

Figure 3.7: Data Acquisition Flowchart(1/2)

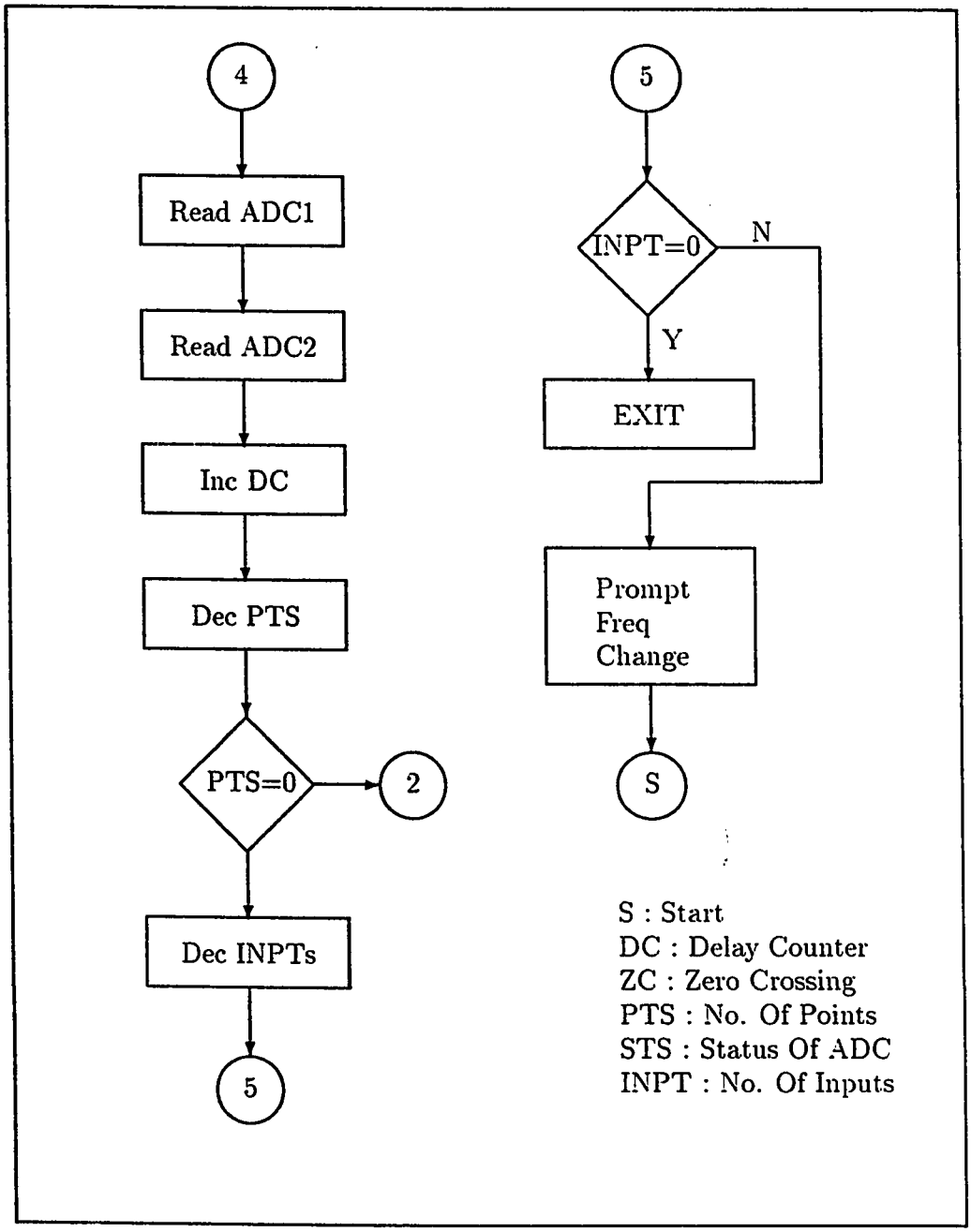

Figure 3.8: Data Acquisition Flowchart(2/2)

The AT-MIO-16L is a high performance, software configurable 12-bit DAQ (data acquisition) board for laboratory, test, measurement, data acquisition and control applications [35]. The board performs high accuracy measurements with high speed setlling to 12 bits. The implementation block diagram is shown in Fig. 3.9

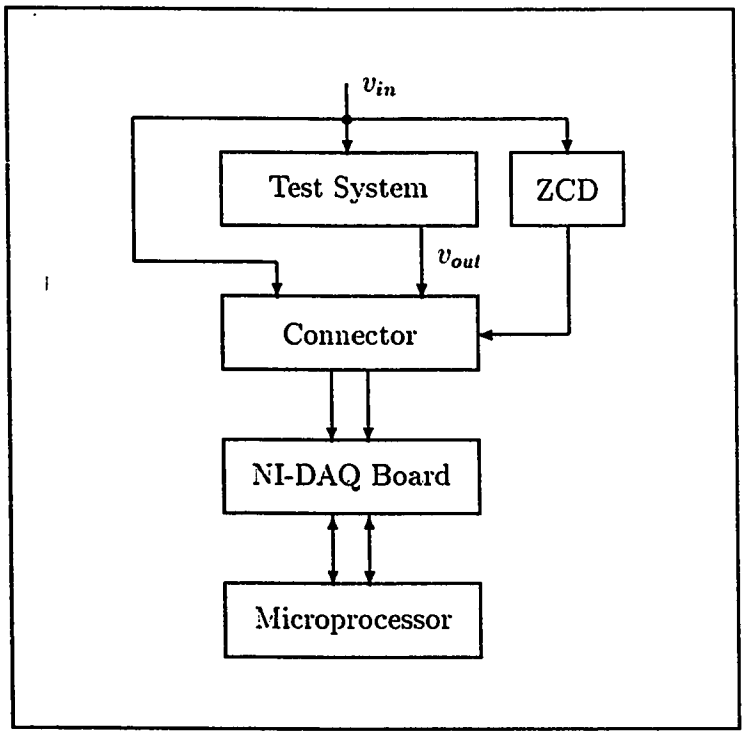

Figure 3.9: Block Diagram of Implementation on NI-DAQ Board

3.9.1 ADC configuration

The board contains an ADC with 9 μ *sec* conversion time. The ADC has 16 channels of input and has software gain settings of 1,10,100 and 500 for low level analog input signals.The board is configured to operate as isolated I/O at a base address of 220 *Hex*.

We have used the board in Differential mode of input for greater accuracy with

an input range of $\pm 10V$.Two channels, CH0 & CH1, of the ADC have been used for input and output respectively. The ADC is operated in the POSTTRIGGER mode. In this mode data acquisition is started after the board receives a hardware triggering signal. This signal is the output of the ZCD, discussed previously.

3.9.2 Circuit Operation

Software for the circuit has been developed in *C language*, using NI-DAQ library functions. The user has only to input the number of input signals and corresponding frequencies, the program calculates the data acquisition rate and prompts him when to change the frequency of input signal. The data corresponding to each frequency is stored in a separate file alongwith the signal frequency.

3.9.3 Circuit Limitations

The ADC is capable of single channel data acquisition of upto 50kHz and for dual channel the limit is 25kHz. These limits are calculated if the data acquisition rate satisfies the Nyquist criterion. The data acquisition rate must be greater than the Nyquist criterion if input-output characteristics are required. We observed that the circuit performance is degraded beyond 12kHz.

Chapter 4

Results & Discussion

4.1 Introduction

We have implemented Abeulma'atti's frequency dependent model. The attempt was to prove the concept presented in the model. In order to validate the model it is necessary to support it with experimental results. The following sections present the overall implementation from characteristic determination to Intermodulation product's amplitude computation. The steps taken to verify the results obtained are also discussed in detail.

Three circuits are presented to verify the implementation, these circuits allow us to verify the frequency independent as well as frequency dependent implementation.

4.2 Operation of Overall Implementation

The process of simulation has been divided into two main parts :

- Acquiring circuit characteristics.
- Modelling & IMP calculation.

Two programs have been developed to implement the above parts. First program acquires the characteristics and stores the data for different frequencies in different

files. The second program takes as input the number of input frequencies and the accuracy required. The process of simulation is subdivided into different routines as follows:

- The input data for each frequency is approximated using Fourier series method to desired accuracy, and the frequency independent coefficients thus generated are stored.
- The stored frequency independent coefficients are approximated using the Fourier series method to generate frequency dependent coefficients.
- User is prompted to provide the amplitudes and frequencies of the signals characterizing the multitone signal.
- From the order of the required intermodulation products at output, a routine calculates the IMP's lying within the band of interest.
- Using the equations for output amplitude calculation and Bessel functions routine the IMP amplitude is calculated and stored.
- A modefied version of the same output calculation routine is used to determine the carrier amplitudes at output.

4.3 Experimental Setup

In order to verify the results obtained from simulation there must exist some means of validation. The results are verified by exciting the circuit using a multitone signal and coupling the output to a spectrum analyzer.

The signal sources should have a minimal harmonic content so that no IMPs are generated due to them. Ideally, the 2nd harmonic should be at -80dB with respect to the amplitude of fundamental frequency. This requires that the sources should be operated at low amplitudes.

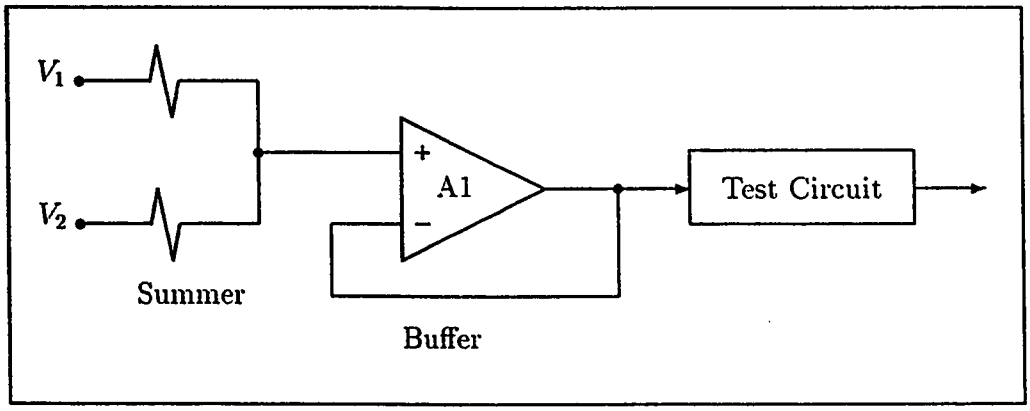

Figure 4.1: Summing & Buffering of Input Signals

In order to excite the circuit by a multitone signal, the signal from different sources must be summed. Hence an ideal summing circuit must be used. If the summer is not ideal it would introduce distortion in the multitone signal. Therefore the amplitudes of the sinusoids used for simulation must be those measured from the spectrum analyzer. The signal sources are summed and then beffered to from the multitone input, Fig. 4.1.

4.4 Measurement of IMPs & Harmonics

We have used a two tone signal to excite the test circuits, since the two tone case is considered important for IMP analysis. Due to the fact that we have monitored the circuit characteristics in a limited band (5kHz-10kHz), we have excited the circuits by all possible combination of sinusoids. The calculated and experimental results are reported along with the error. The resolution of the spectrum analyzer is 0.5kHz on the frequency scale and $1dBV_{rms}$ on the amplitude scale. The results are tabulated and graphically represented. All signal amplitudes are in dBV_{rms} and all frequencies are in kHz.

4.5 Experimental Results

The model implemented can incorporate frequency independent as well as frequency dependent circuits. We have tested the implementation on a number of frequency dependent and frequency independent circuits. Three circuits are presented here:

- Noninverting amplifier
- Low-pass filter
- Band-pass filter

All circuits are designed such that their nonlinear behaviour is observable within the band of frequencies over which the data acquisition can be performed. The input-output characteristics of the circuits are approximated to an accuracy of 1% in all cases and the frequency dependent model is also calculated to the same accuracy.

The measured and calculated IMP amplitudes for different sets of input frequencies and signal amplitudes are tabulated along with their graphical representation. The absolute error has been calculated as:

$$Error = |V_{meas.} - V_{calc.}| \tag{4.1}$$

In all the graphs representing the output spectra the continuous line is the actual output at specified frequency and dashed line is the calculated amplitude at the same frequency. They have been drawn together for the convenience of the reader.

4.5.1 Noninverting Amplifier

To determine the accuracy of the setup for a frequency independent case a noninverting amplifier was implemented. The amplifier is shown in Fig. 4.2.

The gain of the amplifier is given by

$$V_{out} = \left[1 + \frac{R_2}{R_1}\right] V_{in} \tag{4.2}$$

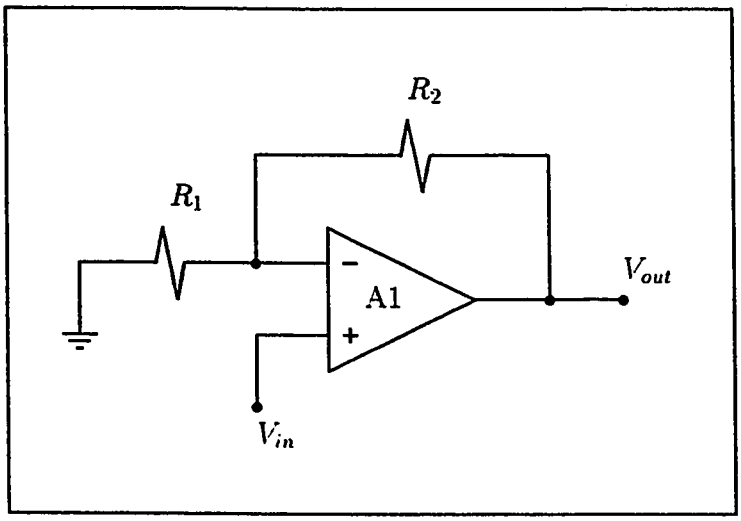

Figure 4.2: Noninverting Amplifier

Cicruit Parameter	Nominal Value
R_1	$1\,K\Omega$
R_2	$2\,K\Omega$
VCC	$+5\,Volts$
VEE	$-5\,Volts$

Table 4.1: Circuit Parameters for Noninverting Amplifier

The different circuit parameters are tabulated in Table 4.1. Frequency response of the circuit as determined from the spectrum analyzer, by a swept tone sinusoid measurement form 0-20kHz, is depicted in Fig. 4.3.

The circuit's instantaneous characteristics were monitiored from 5kHz to 10kHz with a 1kHz step. The circuit was tested for all the possible combinations of two sinusoids from 5-10kHz. The results for the cases which generated maximum IMPs in the band of observation are tabulated and graphically depicted. A picture of the results, Fig. 4.8, obtained from the spectrum analyzer is also included.

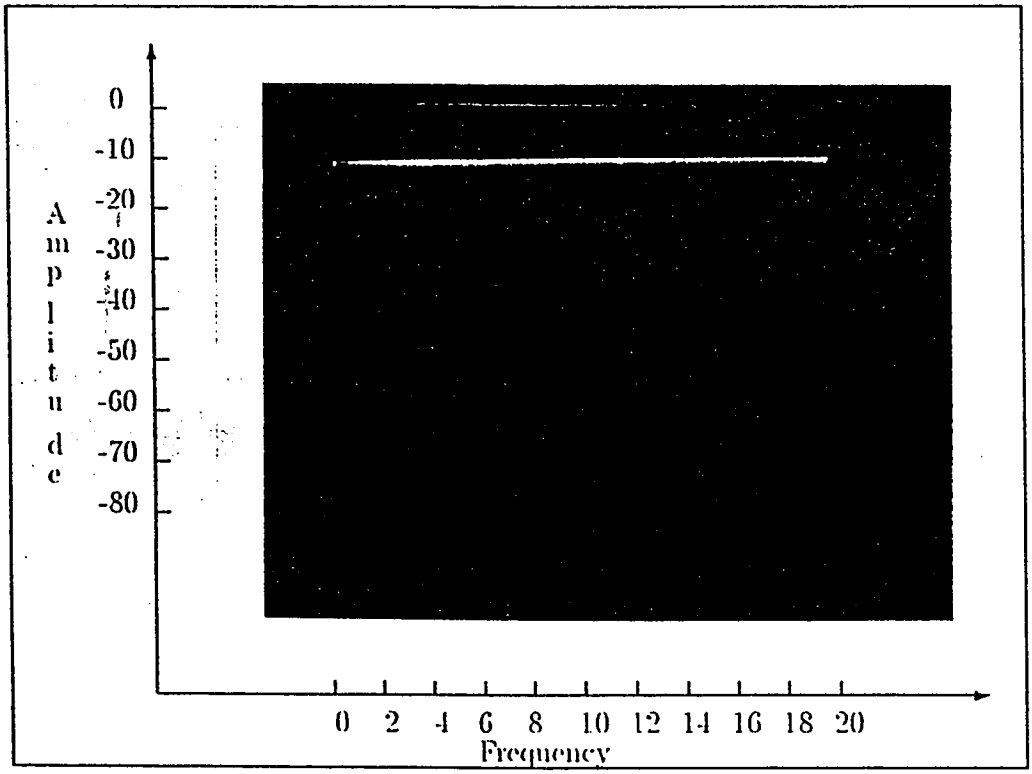

Figure 4.3: Frequency Response of Noninverting Amplifier
Frequency : kHz,-Amplitude : dBV

$f_1 = 7kHz \quad f_2 = 8kHz$			
$V_1 = -8\,dBV \quad V_2 = -8\,dBV$			
Frequency	Measured Amplitude	Calculated Amplitude	Error
7	-2	-2.3	0.3
8	-2	-2.2	0.2
9(IM3)	-58	-57.6	0.4
6(IM3)	-58	-59.2	1.2
5(IM5)	-74	-75.9	1.9
10(IM5)	-76	-75.1	0.9

Table 4.2: IMP & Carrier Amplitudes for Noninverting Amplifier (1/4)
Amplitudes : dBV, Frequency : kHz

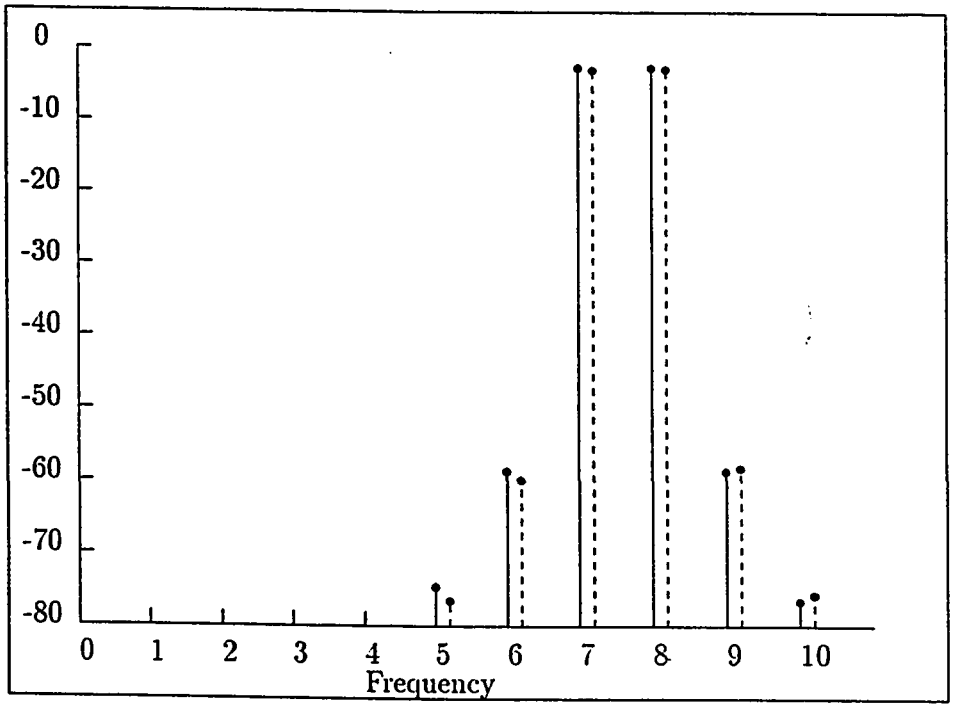

Figure 4.4: Output Spectrum of Noninverting Amplifier (1/4)
Amplitudes : dBV, Frequency : kHz

$f_1 = 7kHz \quad f_2 = 8kHz$			
$V_1 = -10\,dBV \quad V_2 = -10\,dBV$			
Frequency	Measured Amplitude	Calculated Amplitude	Error
7	-4	-4.6	0.6
8	-4	-4.5	0.5
9(IM3)	-58	-59.6	1.6
6(IM3)	-61	-63	2.0
5(IM5)	-68	-69.9	1.9
10(IM5)	-74	-75.1	1.1

Table 4.3: IMP & Carrier Amplitudes for Noninverting Amplifier (2/4)
Amplitudes : dBV, Frequency : kHz

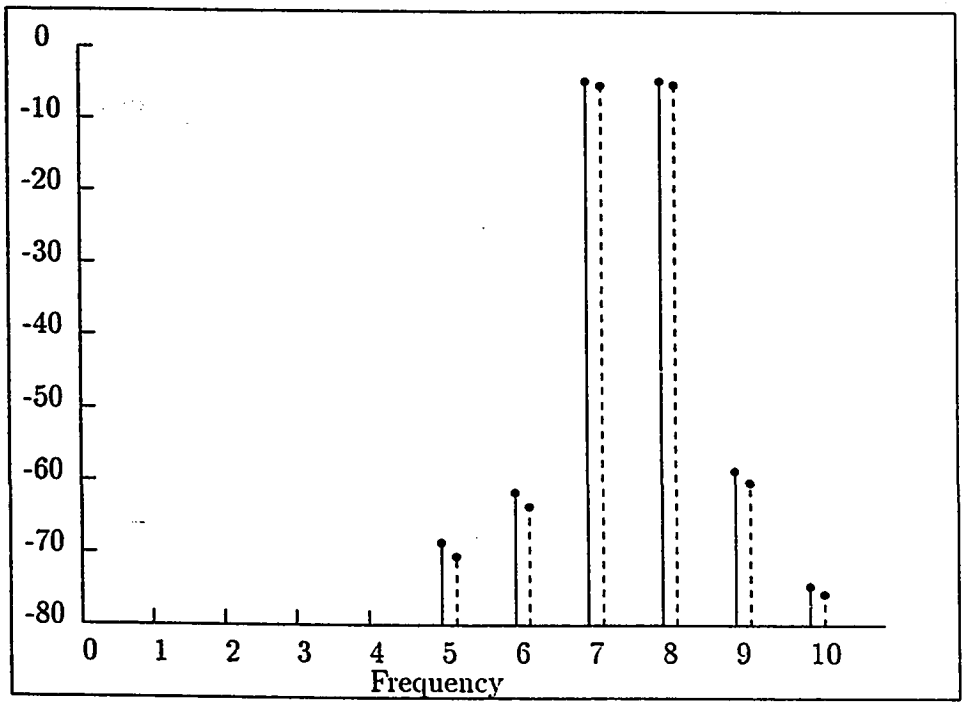

Figure 4.5: Output Spectrum of Noninverting Amplifier (2/4)
Amplitudes : dBV, Frequency : kHz

$f_1 = 8kHz \quad f_2 = 9kHz$			
$V_1 = -8\,dBV \quad V_2 = -8\,dBV$			
Frequency	Measured Amplitude	Calculated Amplitude	Error
8	-2	-2.1	0.1
9	-2	-2.9	0.9
10(IM3)	-55	-53.6	1.4
7(IM3)	-55	-54.8	0.2
6(IM5)	-74	-73.5	0.5

Table 4.4: IMP & Carrier Amplitudes for Noninverting Amplifier (3/4)
Amplitudes : dBV, Frequency : kHz

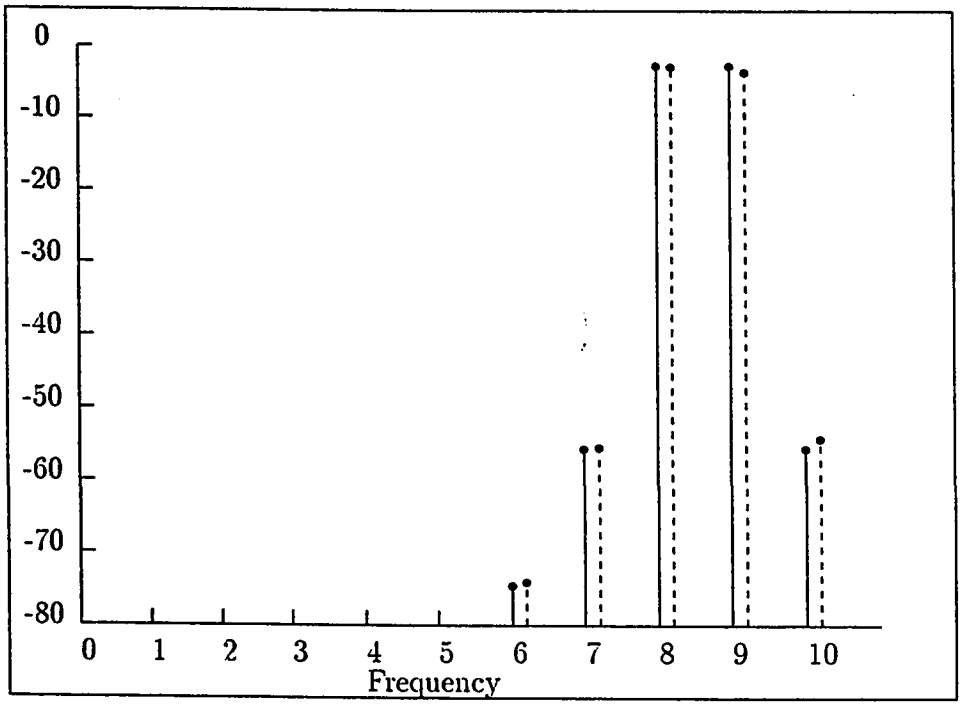

Figure 4.6: Output Spectrum of Noninverting Amplifier (3/4)
Amplitudes : dBV, Frequency : kHz

$f_1 = 6kHz \quad f_2 = 7kHz$			
$V_1 = -8\,dBV \quad V_2 = -8\,dBV$			
Frequency	Measured Amplitude	Calculated Amplitude	Error
6	-2.5	-2.4	0.1
7	-2.0	-2.2	0.2
5(IM3)	-59	-57.6	1.4
8(IM3)	-59	-59.2	0.2
9(IM5)	-74	-72.6	1.4

Table 4.5: IMP & Carrier Amplitudes for Noninverting Amplifier (4/4)
Amplitudes : dBV, Frequency : kHz

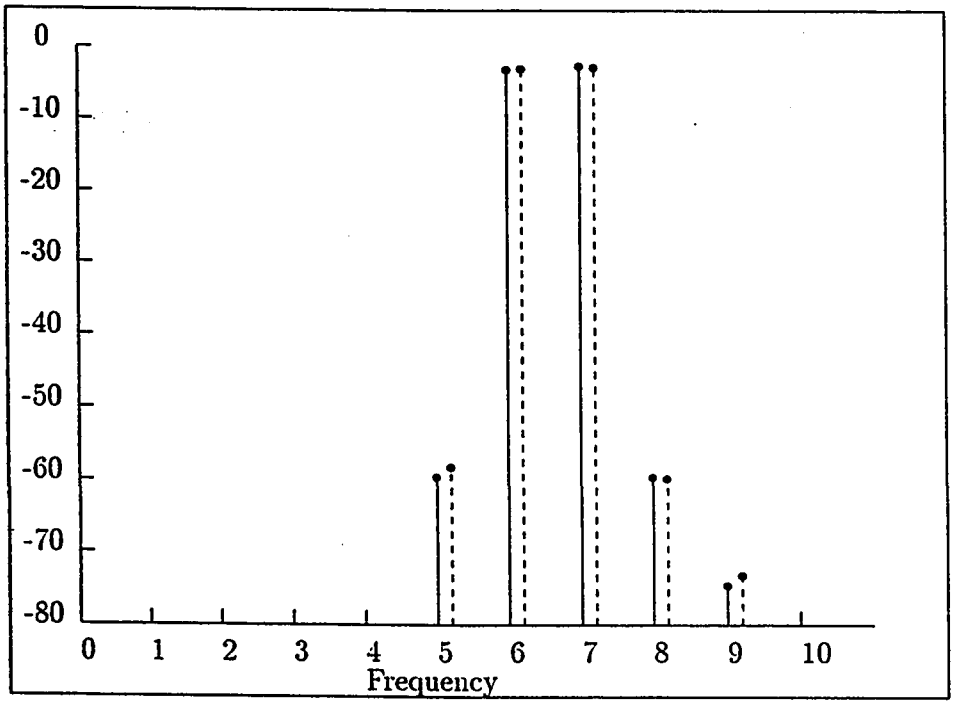

Figure 4.7: Output Spectrum of Noninverting Amplifier (4/4)
Amplitudes : dBV, Frequency : kHz

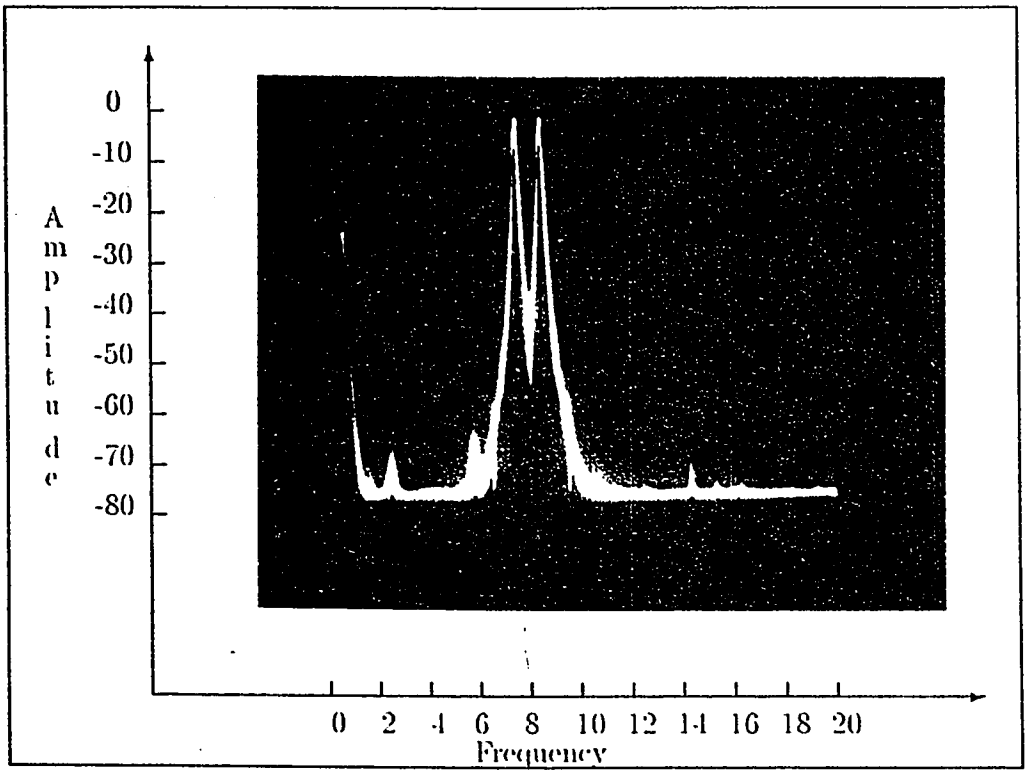

Figure 4.8: Output Spectrum of Noninverting Amplifier
Frequency : kHz, Amplitude : dBV
$f_1 = 7kHz$ $V_1 = -8dBV$
$f_2 = 8kHz$ $V_2 = -8dBV$

Frequency response of the noninverting amplifier's circuit, Fig. 4.3, shows the circuit to be a frequency indpendent circuit from 0kHz to 20kHz. In this case frequency independent coefficients have almost the same amplitude for different frequencies. Hence, the Fourier series method must approximate an almost straight line for generating frequency dependent coefficients. Once the initial offset is removed we are required to approximate a line which is nearly zero for all frequencies. The coefficeints thus generated are of considerably low value and, the model reduces to a frequency independent model.

Tables and graphs for different sets of input frequencies show that the error between actual and calculated readings is less than 3dBs. The gain '2' for the amplifier is easily observable in case of carriers. Our implementation has determined the carrier amplitudes much accurately. For some cases IMPs were observed beyond 10kHz but we have not included them in our results since we did not have data characterizing the device characteristics beyond 10kHz.

4.5.2 Low-Pass Filter

The low pass filter is shown in Fig. 4.9. The cutoff frequency f_o for the filter is 7kHz and the quality factor Q is $\frac{1}{\sqrt{2}}$. The chosen quality factor ensures a maximally flat response. The circuit parameters for the design are given in Table 4.6. Frequency response of the filter and results for different cases are presented in the following tables and figures.

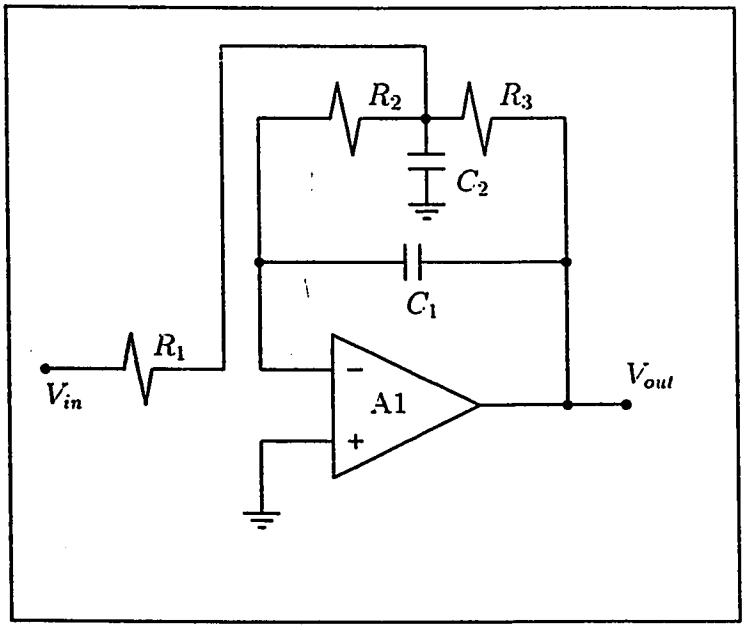

Figure 4.9: Low-pass Filter

Cicruit Parameter	Nominal Value
R_1	45-40 Ω
R_2	45-40 Ω
R_3	45-40 Ω
C_1	$2.2nF$
C_2	$10nF$
VCC	$+15 Volts$
VEE	$-15 Volts$

Table 4.6: Circuit Parameters for Low-pass Filter

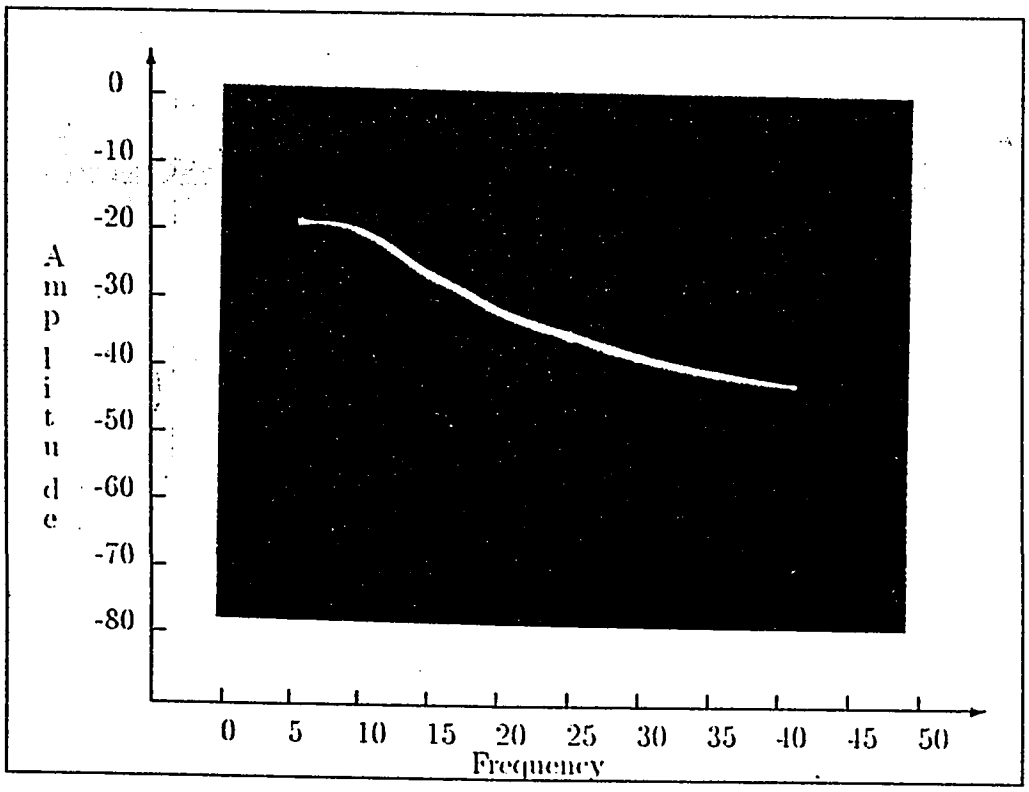

Figure 4.10: Frequency Response of Low-pass Filter
Frequency : kHz, Amplitude : dBV

$f_1 = 7kHz \quad f_2 = 8kHz$			
$V_1 = -10\,dBV \quad V_2 = -10\,dBV$			
Frequency	Measured Amplitude	Calculated Amplitude	Error
7	-6	-7.2	1.2
8	-5	-5.6	0.6
9(IM3)	-61	-62.8	1.8
6(IM3)	-59	-61.2	1.2
5(IM5)	-68	-69.9	1.9
10(IM5)	-69	-70.2	1.2

Table 4.7: IMP & Carrier Amplitudes for Low-pass Filter (1/4)
Amplitudes : dBV, Frequency : kHz

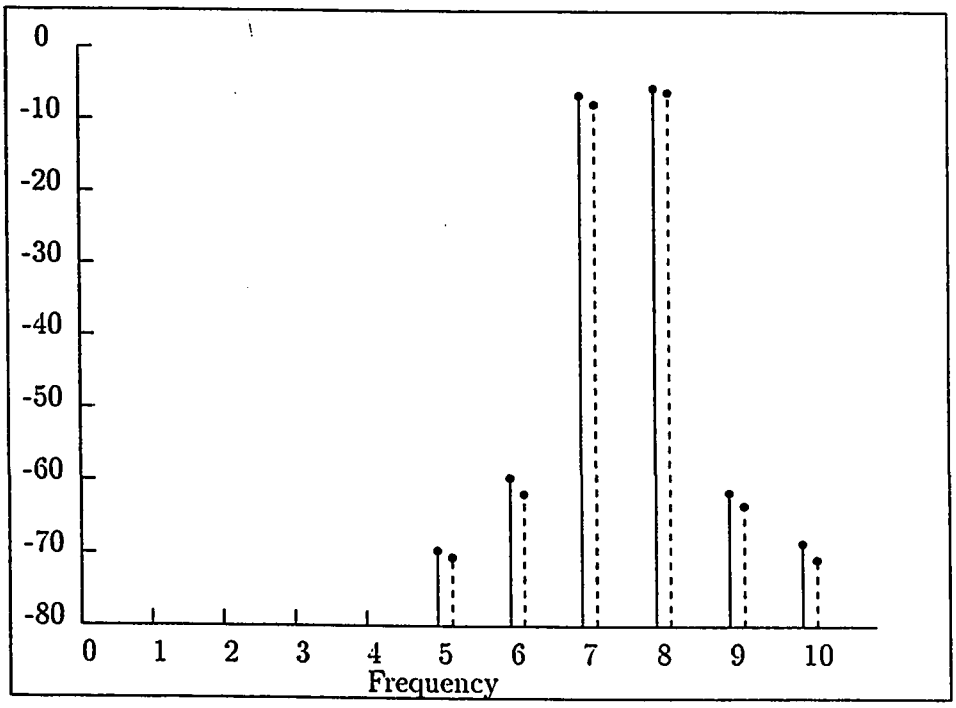

Figure 4.11: Output Spectrum of Low-pass Filter (1/4)
Amplitudes : dBV, Frequency : kHz

$f_1 = 7kHz \quad f_2 = 8kHz$			
$V_1 = -8\,dBV \quad V_2 = -8\,dBV$			
Frequency	Measured Amplitude	Calculated Amplitude	Error
7	-8	-8.6	0.6
8	-8.4	-9.2	0.8
9(IM3)	-59	-57.2	1.8
6(IM3)	-56	-57.9	1.9
5(IM5)	-67	-69.2	2.2
10(IM5)	-65	-67.4	2.4

Table 4.8: IMP & Carrier Amplitudes for Low-pass Filter (2/4)
Amplitudes : dBV, Frequency : kHz

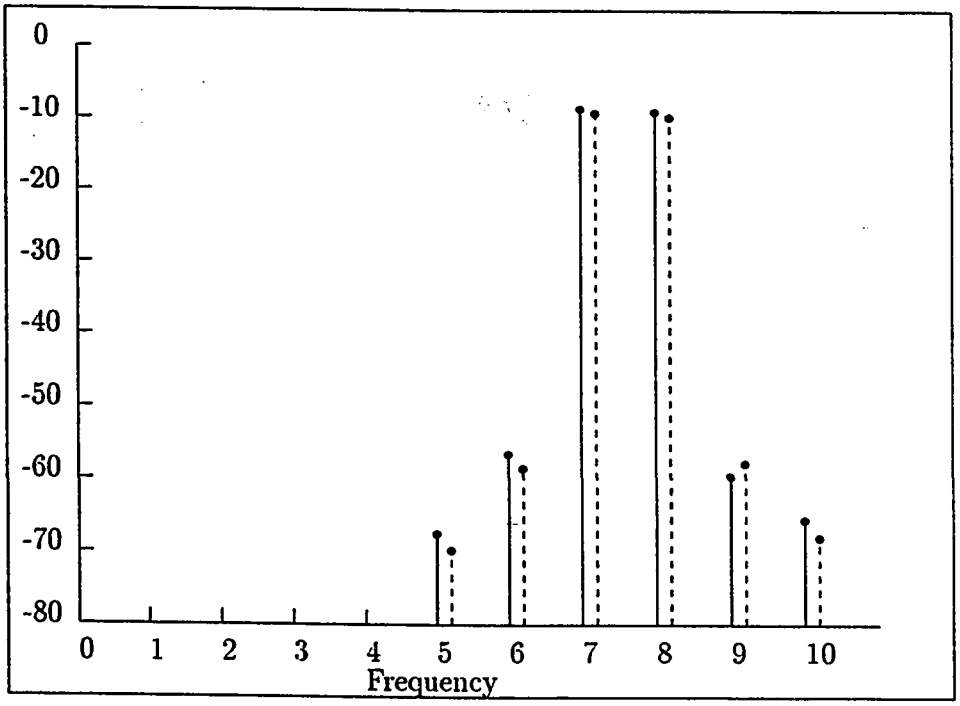

Figure 4.12: Output Spectrum of Low-pass Filter (2/4)
Amplitudes : dBV, Frequency : kHz

$f_1 = 6kHz \quad f_2 = 7kHz$			
$V_1 = -10\,dBV \quad V_2 = -10\,dBV$			
Frequency	Measured Amplitude	Calculated Amplitude	Error
6	-10	-11.4	1.4
7	-9	-10.2	1.2
8(IM3)	-64	-66.2	2.2
5(IM3)	-60	-61.6	1.6
9(IM5)	-72	-73.8	1.8

Table 4.9: IMP & Carrier Amplitudes for Low-pass Filter (3/4)
Amplitudes : dBV, Frequency : kHz

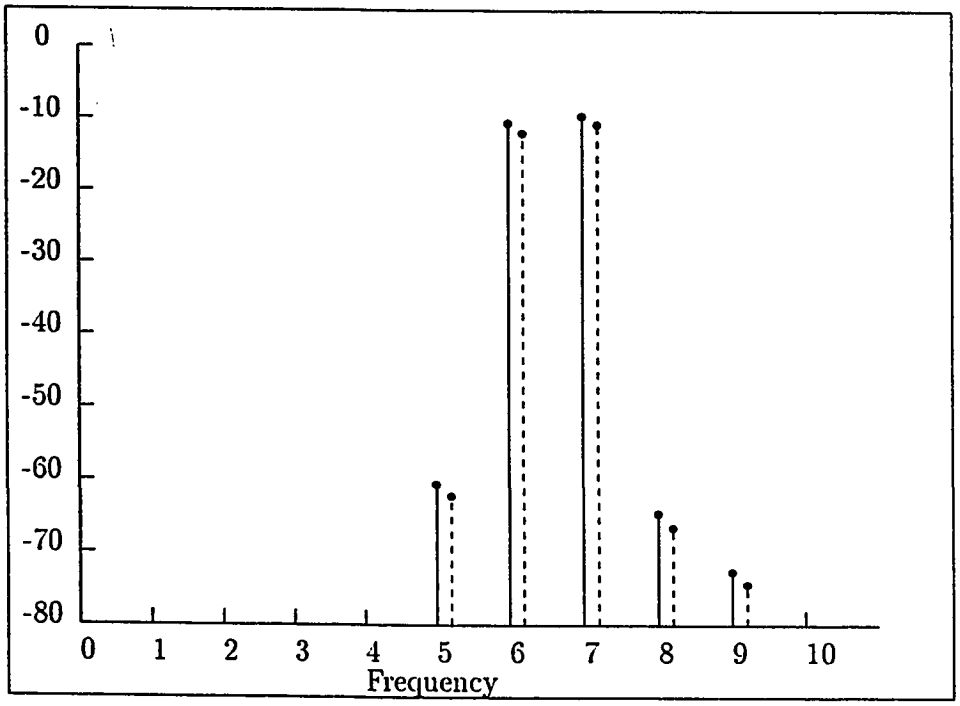

Figure 4.13: Output Spectrum of Low-pass Filter (3/4)
Amplitudes : dBV, Frequency : kHz

$f_1 = 6kHz \quad f_2 = 7kHz$			
$V_1 = -10\,dBV \quad V_2 = -10\,dBV$			
Frequency	Measured Amplitude	Calculated Amplitude	Error
5	-11	-11.8	0.8
6	-10	-10.4	0.4
7(IM3)	-62	-64.6	2.6
8(IM5)	-60	-58.3	1.7

Table 4.10: IMP & Carrier Amplitudes for Low-pass Filter (4/4)
Amplitudes : dBV, Frequency : kHz

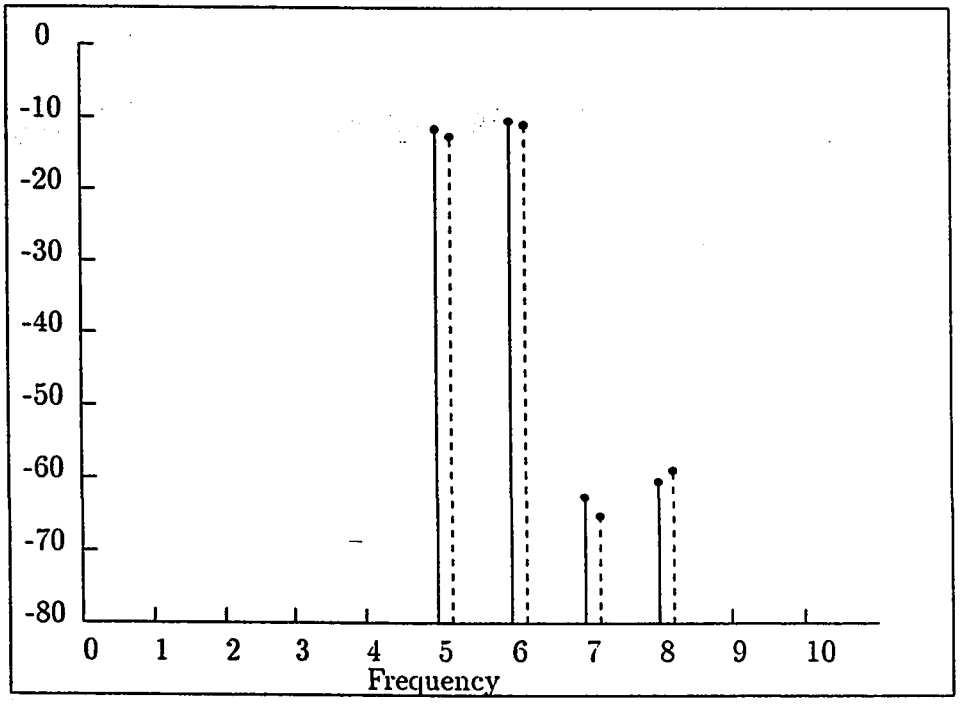

Figure 4.14: Output Spectrum of Low-pass Filter (4/4)
Amplitudes : dBV, Frequency : kHz

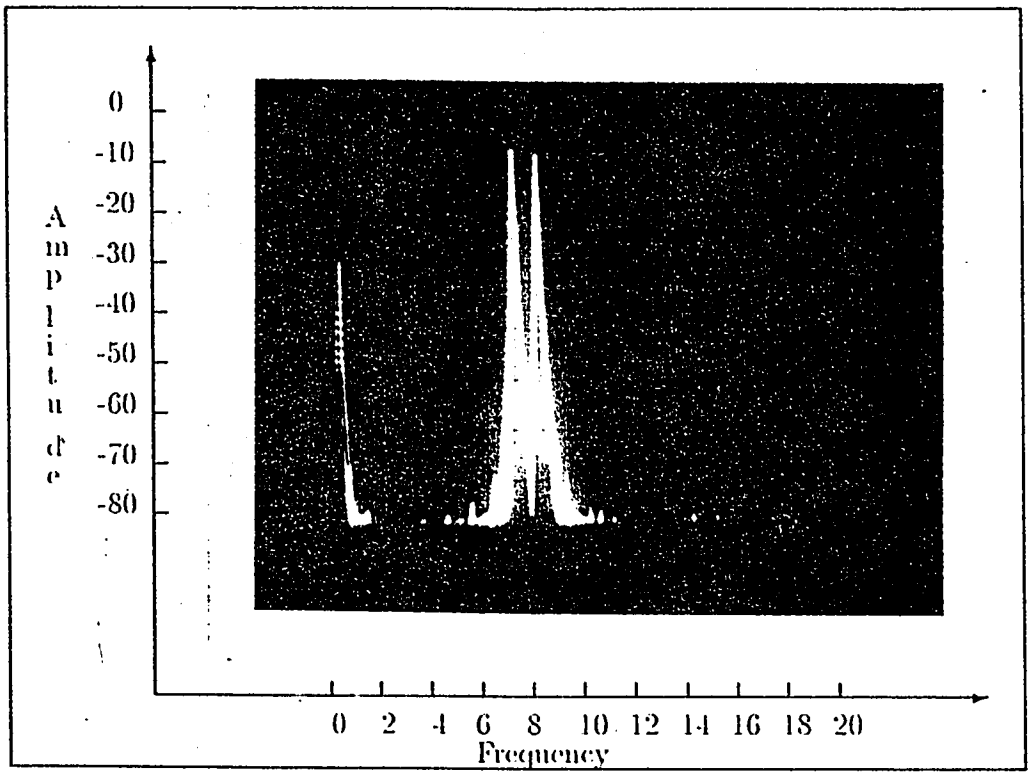

Figure 4.15: Output Spectrum of Low-pass Filter
Frequency : kHz, Amplitude : dBV
$f_1 = 7kHz$ $V_1 = -10dBV$
$f_2 = 8kHz$ $V_2 = -10dBV$

Frequency response of the Low-pass Filter's circuit, Fig. 4.10, shows the circuit to be a frequency dependent circuit. The output amplitude decreases as the frequency of input is increased beyond the cutoff frequency.

The circuit was tested for different combinations of input signals to determine IMPs. The tabulated results show that error is once again less than 3dBs for all cases. The filter has a unity gain in the pass band which, is observable in case of carriers within the passband. Again, for some cases IMPs were observed beyond 10kHz but are not included in the presented results.

4.5.3 Band-Pass Filter

The Band pass filter is shown in Fig. 4.16. The center frequency f_o for the filter is 7kHz and $Q = 5$. This implies that the cut-off frequencies are $f_{lower} = 5kHz$ and $f_{upper} = 9kHz$. The circuit parameters for the design are given in Table 4.11. Frequency response of the filter and results for different cases are presented in the following tables and figures.

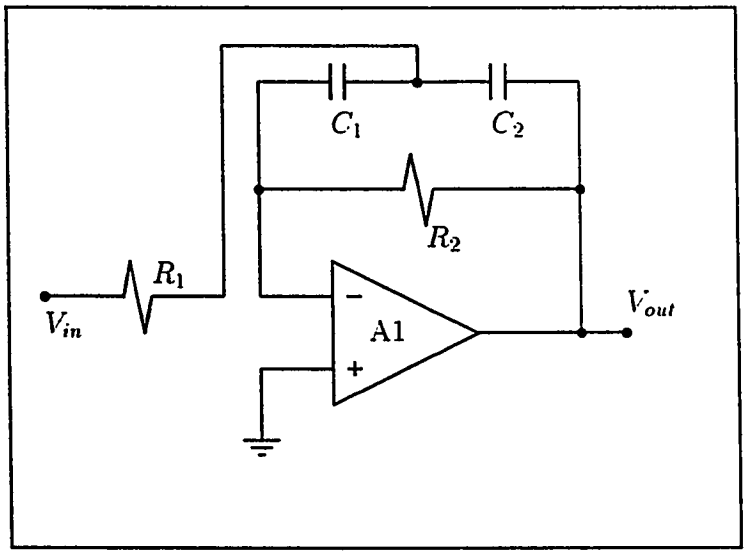

Figure 4.16: Band-pass Filter

Circuit Parameter	Nominal Value
R_1	$632\,\Omega$
R_2	$7750\,\Omega$
C_1	$10nF$
C_2	$10nF$
VCC	$+15\,Volts$
VEE	$-15\,Volts$

Table 4.11: Circuit Parameters for Band-pass Filter

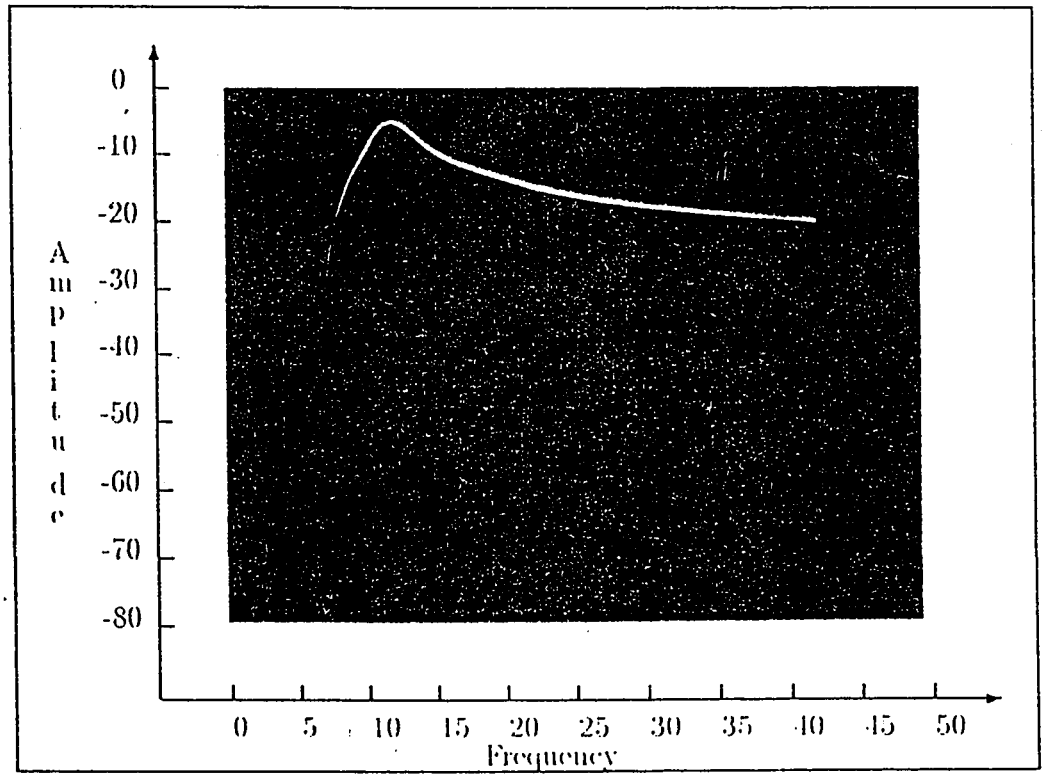

Figure 4.17: Frequency Response of Band-pass Filter
Frequency : kHz, Amplitude : dBV

$f_1 = 7kHz \quad f_2 = 8kHz$			
$V_1 = -20\,dBV \quad V_2 = -20\,dBV$			
Frequency	Measured Amplitude	Calculated Amplitude	Error
7	-6	-6.4	0.4
8	-5.8	-5.3	0.5
9(IM3)	-63	-64.8	1.8
6(IM3)	-62	-60.9	1.1
5(IM5)	-68	-70.2	2.2
10(IM5)	-69	-71.4	2.4

Table 4.12: IMP & Carrier Amplitudes for Band-pass Filter (1/4)
Amplitudes : dBV, Frequency : kHz

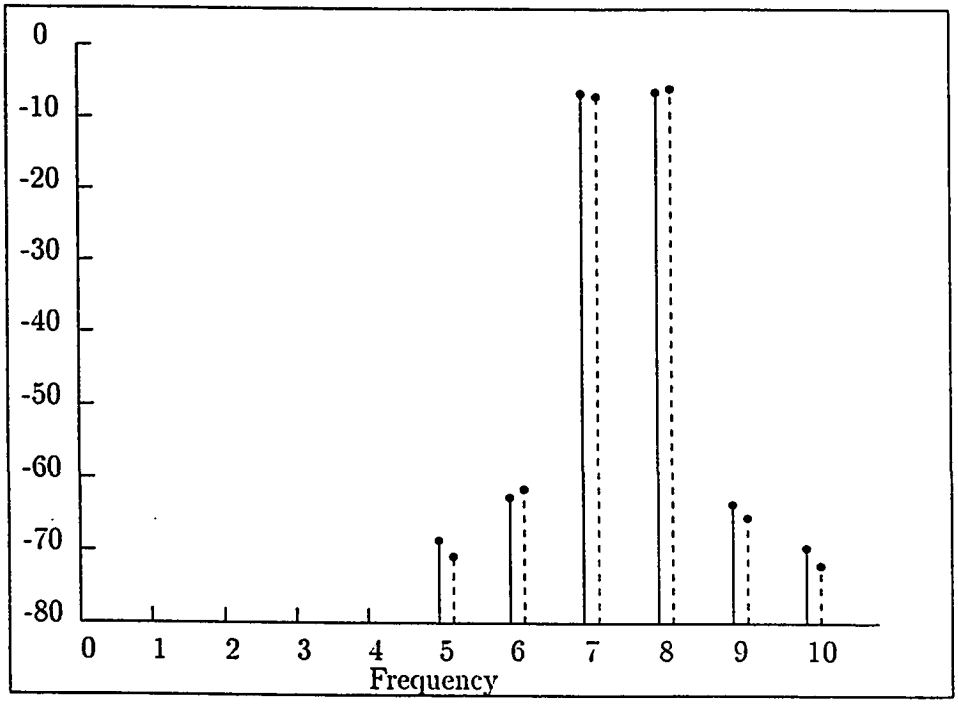

Figure 4.18: Output Spectrum of Band-pass Filter (1/4)
Amplitudes : dBV, Frequency : kHz

$f_1 = 7kHz \quad f_2 = 8kHz$			
$V_1 = -25\,dBV \quad V_2 = -25\,dBV$			
Frequency	Measured Amplitude	Calculated Amplitude	Error
7	-11	-10.5	0.5
8	-10.5	-9.6	0.9
9(IM3)	-58	-60.4	2.4
6(IM3)	-56	-57.9	1.2
5(IM5)	-63	-65.2	2.2
10(IM5)	-65	-63.8	1.4

Table 4.13: IMP & Carrier Amplitudes for Band-pass Filter (2/4)
Amplitudes : dBV, Frequency : kHz

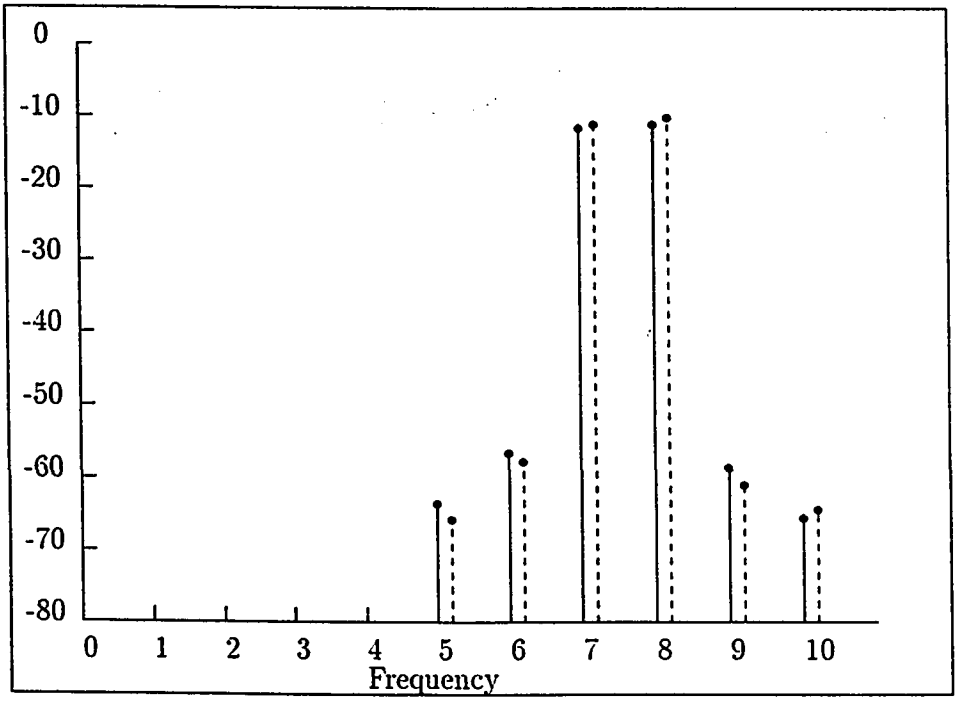

Figure 4.19: Output Spectrum of Band-pass Filter (2/4)
Amplitudes : dBV, Frequency : kHz

$f_1 = 6kHz \quad f_2 = 7kHz$			
$V_1 = -25\,dBV \quad V_2 = -25\,dBV$			
Frequency	Measured Amplitude	Calculated Amplitude	Error
6	-10	-9.5	0.5
7	-10.5	-10.3	0.2
8(IM3)	-56	-54.2	1.8
5(IM3)	-54	-56.1	2.1
9(IM5)	-68	-65.8	2.2

Table 4.14: IMP & Carrier Amplitudes for Band-pass Filter (3/4)
Amplitudes : dBV, Frequency : kHz

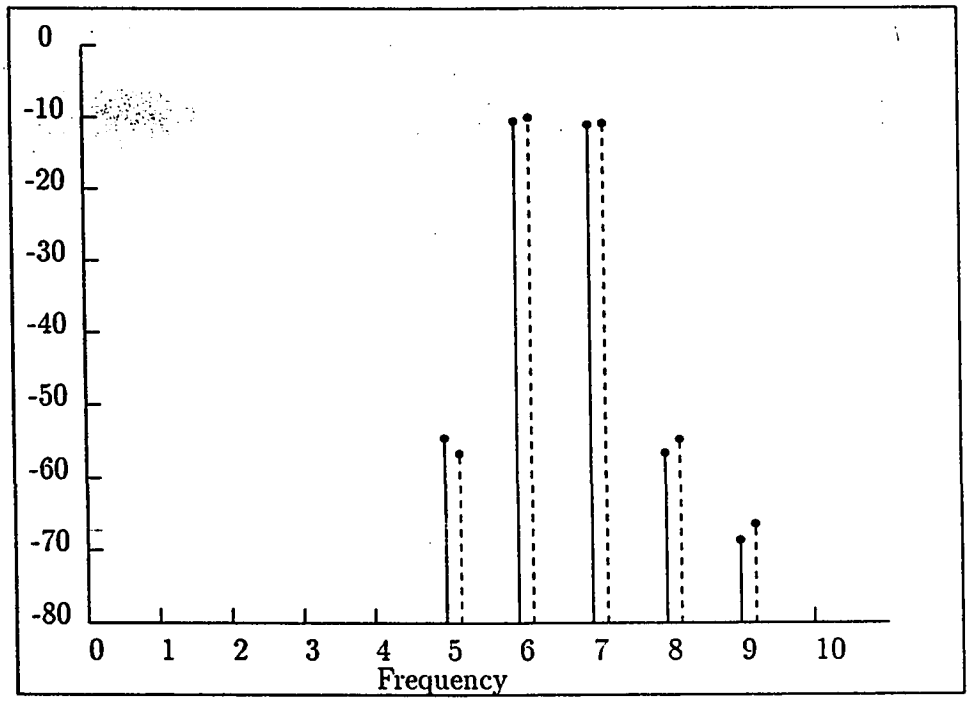

Figure 4.20: Output Spectrum of Band-pass Filter (3/4)
Amplitudes : dBV, Frequency : kHz

$f_1 = 6kHz \quad f_2 = 7kHz$			
$V_1 = -25\,dBV \quad V_2 = -25\,dBV$			
Frequency	Measured Amplitude	Calculated Amplitude	Error
5	-11	-11.2	0.2
6	-10	-10.4	0.4
7(IM3)	-60	-62.1	2.1
8(IM5)	-64	-65.6	1.6

Table 4.15: IMP & Carrier Amplitudes for Band-pass Filter (4/4)
Amplitudes : dBV, Frequency : kHz

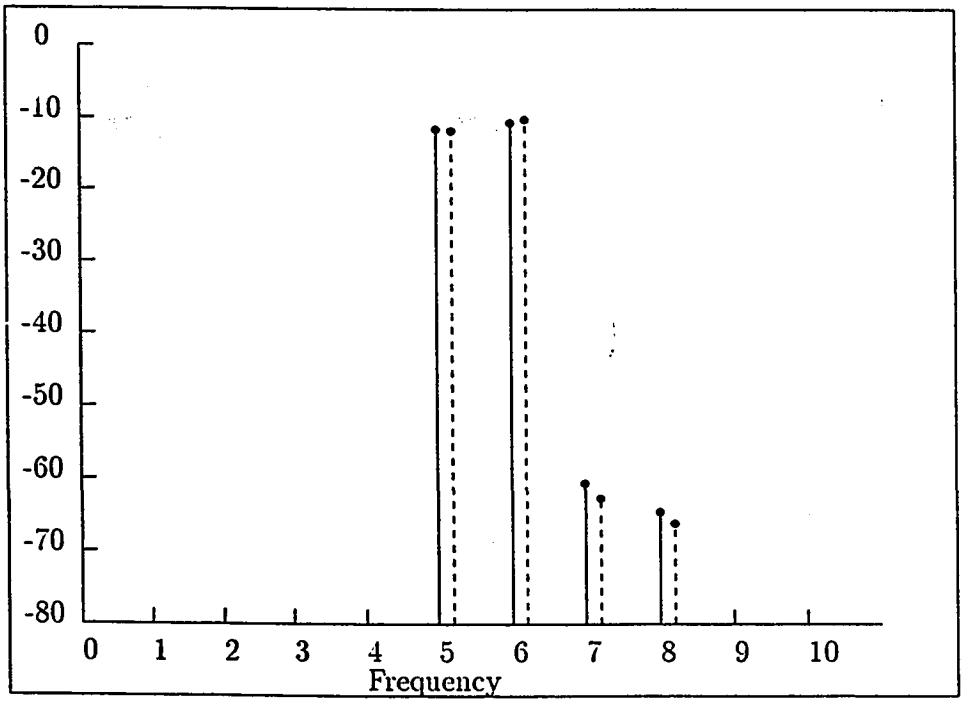

Figure 4.21: Output Spectrum of Band-pass Filter (4/4)
Amplitudes : dBV, Frequency : kHz

From Fig. 4.17 circuit (band-pass filter) is a frequency dependent circuit, Fig. 4.17. As expected, the frequency independent coefficients are found to be of band-pass nature. These coefficeints are easily approximated by the Fourier series approximation. Since, the frequencies over which the data acquisition was performed were limited from 5kHz to 10kHz we applied all the possible two tone combinations to the circuit. The results show the absolute error to be less than 3dBs.

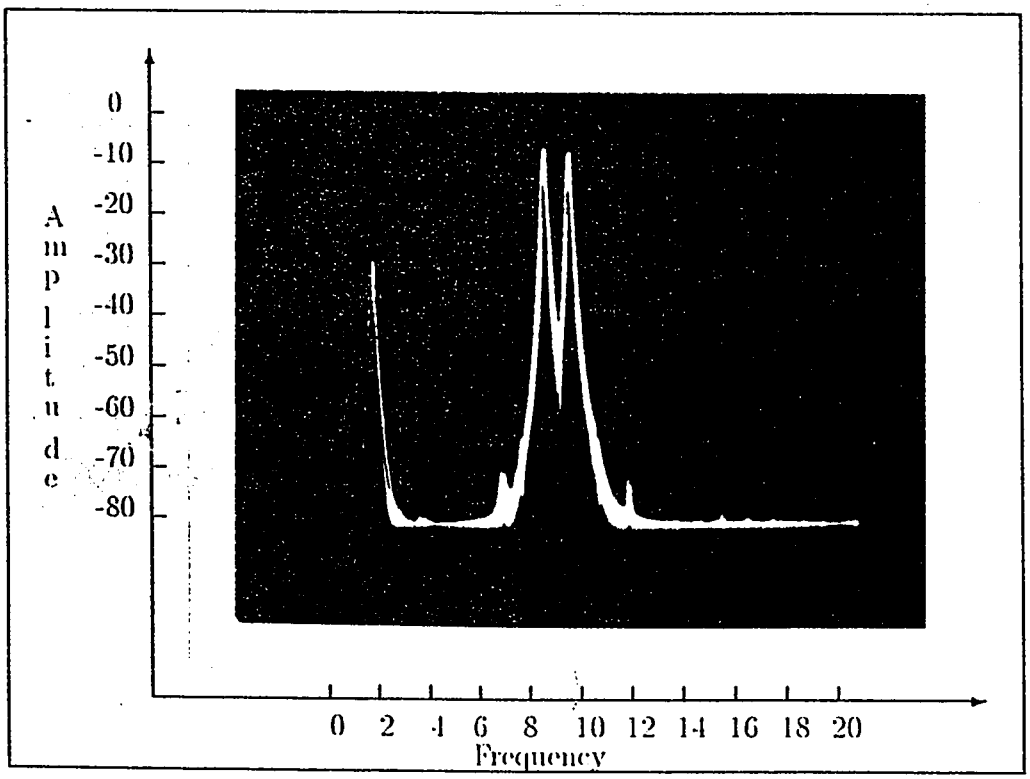

Figure 4.22: Output Spectrum of Band-pass Filter
Frequency : kHz, Amplitude : dBV
$f_1 = 7kHz$ $V_1 = -25dBV$
$f_2 = 8kHz$ $V_2 = -25dBV$

4.6 Discussion of Error

In all practical implementations one has to live with a certain amount of error. The error (absolute) reported for all the circuits is less than $3dB$. As reported by Abuelma'atti [30] this amount of error is tolerable in practical applications. This error can be attributed to the following factors:

- Round off error due to multiple computations.
- ADC quantization error.
- Measurement error from spectrum analyzer.
- Frequency dependent coefficients require large number of coefficients.
- Assumption that characteristics are odd.

The error due to the Fourier series approximation when it is used for frequency dependent coefficients and odd characteristics assumption is discussed in detail in the following subsections.

4.6.1 Applicability of Fourier series Approximation

The Fourier series method has been used to approximate the characteristics and the resulting frequency independent coefficients for frequency dependent model are also generated by the same method. The method is ideal for simulation of saturating functions. Before approximating the fr-equency independent coefficients it is required that the number of coefficients for different characteristics be equalized. This means that same number of coefficients must be used for approximating each input-output characteristic. This is a requirement imposed by the parallel model.

The equalization process can at times result in a situation as depicted in Fig. 4.23. The Fourier series method requires a large number of coefficients to approxi-

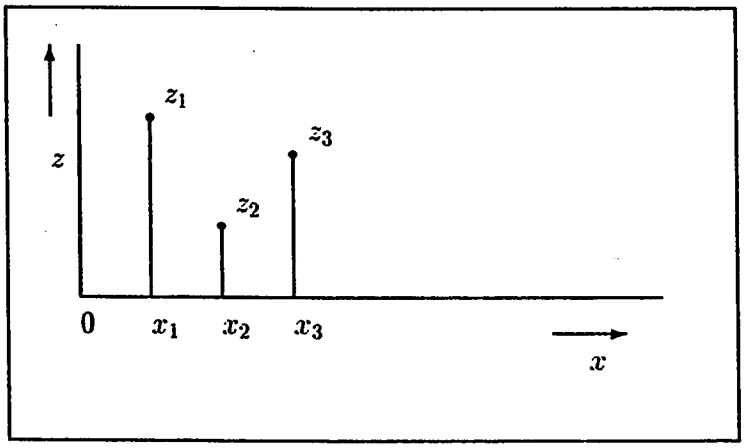

Figure 4.23: Sample Data case

mate such data. Since dimension of an array must be defined in a program beforehand. This implies that we can be faced with a situation in which the frequency dependent coefficients will not be calculated to the required degree of accuracy. In such a case, the approximation is repeated and the coefficients are selected such that the resulting error is as close to the specified accuracy as possible. This contributes to the overall error in the IMP amplitudes.

4.6.2 Odd Order Characteristics

For all practical circuits it is observed that the saturation in one direction is not exactly mirrored in the other direction. This implies that assuming the device characteristics to be odd is unfair because the output will contain even order IMPs as well. If these IMP's lie at the same frequency as that of an other IMP or a carrier it results in an error.

Chapter 5

Conclusions & Recommendations for Future Work

5.1 Introduction

In this thesis we have implemented the frequency dependent model of Abuelma'atti [15]. The overall implementation has been tested on a number of circuits and the results have been presented in the last chapter. In this chapter we will draw some conclusions regarding this work and outline the limitations of the implementation. We will then discuss possible extensions of the work and areas of future work.

5.2 Conclusions

The motivation behind the work was to prove the concept of the frequency dependent model presented by Abuelma'atti [15]. The model along with the required routines has been implemented. An automatic characteristic measuring system was implemented that computed the input-output instantaneous characteristics at different frequencies. This data was then used to construct the frequency dependent model of the device. We have presented results that validate the frequency independent and frequency dependent behaviour of the model. The implementation discussed in the last chapters can serve as prototype for an integrated system to compute IMP

amplitudes at the output of a device.

5.2.1 System Limitations

We were faced by some limitations which we feel should be addressed to in future applications.

- The main limitation has been the data acquisition speed. The system implemented by us could operate at relatively low frequencies (up to 12kHz only).
- The implemented Fourier series routine had the disadvantage of requiring large number of coefficients for frequency dependent model computation in some cases.

5.3 Recommendations for Future Work

At the end of this thesis we feel that there is room for improvement. We have proved the concept and suggest that:

- The implementation should be extended to incorporate high frequency signals. This would require that a dedicated system be implemented that has the capability to operate at high frequencies.
- A generalized Fourier series routine may be the used to approximate the input-output characteristics. This will enable the user to compute the odd as well as even IMPs.
- The software can be extended to include a routine for generating a warning signal when an IMP is falling on the same frequency as that of the carrier. The degradation introduced by such an IMP should also be recorded.
- The hardware implementation should be enhanced to include a correction facility to ensure proper operation of the device.

The possibility of having an integrated systen that can perform online correction to the system can enable the designer with a high degree of freedom. The implementation can provide him data about the test system before it becomes a part of a complex circuit. The implemenation can be used in a stand alone configuration and can operate in remote locations. The IMP data can be transmitted to a base station where the operation can be easily monitored, examples of such a situation are satellites, offshore installations and remote transmitting stations.

Bibliography

[1] M.K.Scherba and J.E.Rowe. Characteristics of Multisignal and Noise-modulated High-Power Microwave Amplifiers. *IEEE Transactions on Electronic Devices*, pages 11–34, January 1971.

[2] O.Shimbo, J.C.Fuenzalida, and W.L.Cook. Time Domain Analysis of Intermodulation Effects Caused by Nonlinear Amplifiers. *Cornsat Technical Review*, 3(1), 1973.

[3] S.Benedetto. *Digital Transmission Theory.* Prentice Hall Publications Corporation, Englewood Cliffs NJ(USA), 1987.

[4] N.M.Blachman. Detectors,Bandpass Nonlinearities and their Optimization: Inversion of Chebyshev Transform. *IEEE Transactions on Information Theory*, IT-17(4):398–404, July 1971.

[5] V.Volterra. *Theory of Functions and Integrals and Integro-Differential Equations.* New York: Dover, 1959.

[6] S.P.Boyd. *Volterra series:Engineering Fundamentals.* Phd Dissertation, University of California, Berkley, 1985.

[7] K.Y.Chang. Inter Modulation Noise and Products Due to Frequency Dependent Nonlinearities in Catv Systems. *IEEE Transactions on Communications*, COM-23(1):142–155, January 1975.

[8] Y.Hu, J.C.Mollier, and J.Obregon. A New Method of Third Order Intermodulation Reduction in Nonlinear Microwave Systems. *IEEE Transactions on Microwave Theory and Techniques*, MTT-34(2):245–250, February 1986.

[9] G.L.Heiter. Characterisation of Nonlinearities in Microwave Devices and Systems. *IEEE Transactions on Microwave Theory and Technology*, MTT-34(12):795–805, December 1973.

[10] M.C.Jeruchim and R.Blum. Modelling Nonlinear Amplifiers for Communication Simulation. *International Conference on Communication*, pages 1468–1472. 1989.

[11] M.J.Eric. Intermodulation Analysis of nonlinear Devices for Multiple Carrier Inputs. *Communication Research Center,CRC Report*, 1234, 1972. Ottawa,Canada.

[12] P.Hetrakul and D.P.Taylor. Nonlinear Quadrature model for a Travelling wave tube-type Amplifier. *Electron Letters*, 11(2):50, 1975.

[13] H.B.Poza. A Wideband Data Link Computer Simulation Model. *Proceedings of NAECON Conference*, 1975.

[14] A.A.M.Saleh. Frequency Independent and Frequency Dependent models of TWT Amplifiers. *IEEE Transactions on Communication*, COM-29(11):1715–1720, November 1981.

[15] M.T.Abuelma'atti. Frequency Dependent Nonlinear Quadrature Model for TWT Amplifiers. *IEEE Transactions on Communications*, COM-32(8):982–986, August 1984.

[16] N.G.Riley, M.Gallagher, and K.V.Prasad. A Simple Model of Intermodulation Spectra for use on a Personal Computer. *IEE International Conference on Electromagnetic Compatibility*, pages 99–102, 1990. Publ. No. 326.

[17] Frank Box. Analysis of Intermodulation Relationships Within a Limited Band of Interest. *IEEE Transactions on Communications*, COM-27:1226–1230, 1979.

[18] M.T.Abuelma'atti and J.G.Gardiner. Approximate Method for Hand Computation of Amplifier Intermodulation Product Levels. *IEE Proceedings*, 128 Pt.G(1):32–34, February 1981.

[19] M.T.Abuelma'atti and J.G.Gardiner. Input Power Assignment of Equal-Amplitude Multicarrier Systems for given Carrier Power. *International Journal of Electronics*, 50:55–60, 1981.

[20] M.R.Smith. Intermodulation, Differentiation, Data Smoothing, and Least Square Fit to Data with Decreased Computational Overhead. *IEEE Transactions on Industrial Electronics*, 32:135–141, 1985.

[21] L.A.Pipes and L.R.Harvill. *Applied Mathematics for Engineers and physicists.* New York: McGraw Hill, 1970.

[22] R.L.Burden and J.D.Faires. *Numerical Analysis.* Prindel, Weber & Schmidt, Boston, Massachusetts, 1981.

[23] I.A.Dodes. *Numerical Analysis for Computer Science.* New York: Elsevier North Holland, 1978.

[24] R.W.Hamming. *Numerical Methods for Scientists and Engineers.* New York: McGraw Hill, 1962.

[25] M.T.Abuelma'atti. A Simple Algoritm for Fitting Measured Data to Fourier series Models. *International Journal of Mathematics*, 26(1):107–112, 1993.

[26] E.Kreyszig. *Advanced Engineering Mathematics.* New York: John Wiley, 1979.

[27] C.D.McGillen and G.R.Cooper. *Continuous and Discrete Signal and System Analysis.* New York: CBS, 1986.

[28] M.J.Maron. *Numerical Analysis, A Practical Approach.* New York: Macmillan, 1987.

[29] A.C.Heathman. *Methods of Intermodulation Prediction in Communications Systems.* Phd Dissertation, University of Bradford, U.K, 1979.

[30] M.T.Abuelma'atti. *Reduction of Intermodulation in Communications Amplifiers by Pre-correction Techniques.* Phd Dissertation, University of Bradford, U.K, 1979.

[31] R.A.Waldron. Formulas for Computation of Approximate Values of Some Bessel Functions. *IEEE Proceedings*, 69(12):1686–1588, December 1981.

[32] M.Abramowitz and I.A.Stegun. *Handbook of Mathematical Functions.* New York : Dover, 1965.

[33] A.S. Sedra and K.C.Smith. *Microelectronic Circuits.* Saunders College Publishing, 1991.

[34] W.A.Triebel and A.Singh. *The 8088 and 8086 Microprocessors, Programming, Interfacing, Software, Hardware, and Applications.* Prentice Hall, Englewood Cliffs,New Jersey, 1990.

[35] National Instruments. *AT-MIO-16 User Manual.* NI-DAQ, 1993.

Vita

- Rizwan Ali Tiwana
- Born in Lahore, Pakistan
- Received Bachelor's degree in Electrical Engineering from the University of Engineering and Technology, Lahore, Pakistan in September, 1992.
- Completed Master's degree requirements at King Fahd University of Petroleum and Minerals, Dhahran, Saudi Arabia in December, 1994.